

1

2

3 **Fork Pausing Complex Engages Topoisomerases at the Replisome**

4

5 Maksym Shyian^{*}, Benjamin Albert, Andreja Moset Zupan, Vitalii Ivanitsa, Gabriel Charbonnet, Daniel Dilg, and

6 David Shore^{* α}

7 Department of Molecular Biology and Institute of Genetics and Genomics of Geneva (iGE3), University of

8 Geneva, Geneva 4, 1211 Switzerland

9

10 Running title: Replication fork sTOP model

11

12

13 ^{*}Corresponding authors: Maksym.Shyian@unige.ch; David.Shore@unige.ch.

14 ^{α} Lead contact

15

16

17 **ABSTRACT**

18 Replication forks temporarily or terminally pause at hundreds of hard-to-replicate regions around the
19 genome. A conserved pair of budding yeast replisome components Tof1-Csm3 (fission yeast Swi1-Swi3 and
20 human TIMELESS-TIPIN) acts as a ‘molecular brake’ and promotes fork slowdown at proteinaceous
21 replication fork barriers (RFBs), while the accessory helicase Rrm3 assists the replisome in removing protein
22 obstacles. Here we show that Tof1-Csm3 complex promotes fork pausing independently of Rrm3 helicase by
23 recruiting topoisomerase I (Top1) to the replisome. Topoisomerase II (Top2) partially compensates for the
24 pausing decrease in cells when Top1 is lost from the replisome. The C-terminus of Tof1 is specifically
25 required for Top1 recruitment to the replisome and fork pausing but not for DNA replication checkpoint
26 (DRC) activation. We propose that forks pause at proteinaceous RFBs through a ‘sTOP’ mechanism (‘slowing
27 down with TOpoisomerases I-II’), which we show also contributes to protecting cells from topoisomerase-
28 blocking agents.

29

30 **Keywords:** Tof1, Csm3, Mrc1, topoisomerase, Top1, Top2, RFB, replisome, replication fork pausing

31

32 INTRODUCTION

33 The chromosomal DNA of most cells is duplicated once per cell cycle due to the concerted action of
34 DNA helicases unwinding the DNA template, topoisomerases unlinking the parental strands, and DNA
35 polymerases synthesizing the daughter strands in collaboration with a myriad of accessory factors (Bell and
36 Labib 2016). This assembly of proteins on the DNA replication fork is called the ‘replisome’. In order to
37 achieve the completeness of genome duplication, the replisome should pass through the entirety of all
38 chromosomes. On average budding yeast replisomes move through ca. 20 kb of DNA before merging with a
39 converging fork (Pasero et al. 2002). However, *in vivo* the speed of the replisome is not uniform, as it
40 temporarily or terminally slows/pauses/arrests/stalls at certain locations, called replication fork barriers
41 (RFBs). RFBs are comprised by ‘unconventional’ DNA structures (inverted repeats, trinucleotide repeats, G4
42 quadruplexes), RNA/DNA hybrids (R-loops), and tight protein/DNA complexes (Gadaleta and Noguchi 2017).
43 Examples in yeast of the latter type of RFB are found at the rDNA repeat array, tRNA genes (tDNA),
44 telomeres, centromeres, silent mating type loci (*HML/HMR*) silencer elements, and dormant origins of
45 replication (Gadaleta and Noguchi 2017).

46 Replisome pausing at these protein barriers involves two components: (1) a tight DNA-binding
47 protein block specific for a given locus (e.g. Fob1 (rDNA RFB - rRFB), the RNA polymerase III pre-initiation
48 complex, the general regulatory factor Rap1, or the origin recognition complex) and (2) a “fork
49 pausing/protection complex” (FPC) – the evolutionary conserved heterodimer represented by Tof1-Csm3 in
50 budding yeast (Swi1-Swi3 in fission yeast and TIMELESS-TIPIN in human). Tof1-Csm3 is also found in
51 association with Mrc1 (not itself involved in replication pausing) in a trimeric complex referred to as MTC,
52 which travels with other factors in a still larger assembly on replication forks called the Replisome
53 Progression Complex (RPC) (Gambus et al. 2006). Loss of Tof1-Csm3 leads to a decrease in replisome pausing
54 at many of the studied protein barriers in budding and fission yeast, and human cells (Gadaleta and Noguchi

55 2017), while increasing blockage at some unconventional DNA structures (Voineagu et al. 2008). Accessory 5'
56 to 3' DNA helicase Rrm3 is a part of the yeast replisome and uses its ATPase/helicase activity to assist the
57 main replicative 3' to 5' CMG helicase (Cdc45-Mcm2-7-GINS) in progression specifically at the protein blocks
58 (Ivessa et al. 2000; Ivessa et al. 2003; Azvolinsky et al. 2006). Replication fork stalling is proposed to fuel
59 tumorigenesis and ageing (Gaillard et al. 2015). However, the molecular mechanism of action of the Tof1-
60 Csm3, Rrm3 and replisome progression through protein blocks is complex and incompletely understood.

61 In addition to helicases, the replisome must employ topoisomerases in order to topologically unlink,
62 or swivel, the two parental DNA strands (Duguet 1997). Topoisomerase I (Top1 in budding yeast) is regarded
63 as the main replicative swivelase, while topoisomerase II (yeast Top2) provides a back-up mechanism when
64 Top1 is not available (Kim and Wang 1989a; Bermejo et al. 2007). It was postulated that similarly to
65 helicases, topoisomerase action should be impeded by the presence of tight protein complexes on DNA in
66 front of the fork (Keszthelyi et al. 2016).

67 We set out here to understand the mechanism of Tof1-Csm3-dependent replisome arrest/pausing at
68 RFBs. We show first that the Tof1-Csm3 fork pausing complex acts independently of the accessory helicase
69 Rrm3. Instead, we find that Tof1-Csm3 engages replicative topoisomerase I (and backup topoisomerase II) at
70 the replisome to promote fork pausing at proteinaceous RFBs (sTOP mechanism). The Tof1 C-terminus
71 mediates Top1 association with the replisome and fork pausing but is not required for the DNA replication
72 checkpoint (DRC). sTOP and DRC mechanisms jointly promote cellular resistance to topoisomerase-blocking
73 agents.

74

75 RESULTS

76 ***Fork pausing complex Tof1-Csm3 acts independently of Rrm3 helicase***

77 Replication forks slow down at hundreds of tight protein/DNA complexes around the yeast genome
78 (Gadaleta and Noguchi 2017). In search for the fork pausing mechanism, we started by first confirming with
79 2D and 1D gels (Brewer and Fangman 1988; Kobayashi et al. 2004) that only Tof1-Csm3 but not Mrc1
80 (Tourriere et al. 2005; Hodgson et al. 2007) or other related RPC components are required for fork pausing at
81 the rRFB (**Fig. 1A, S1A-C**). Accessory helicase Rrm3 helps the replisome to move past protein RFBs
82 throughout the genome (Ivessa et al. 2003). Upon initial characterization of the roles of Tof1 and Csm3 in
83 fork pausing using 2D gels, it was postulated that they work by counteracting the Rrm3 helicase (**Fig. 1A,**
84 model '1') (Mohanty et al. 2006; Bairwa et al. 2011). If this were true, fork pausing should become
85 completely independent of Tof1-Csm3 in cells lacking Rrm3. However, closer inspection of the 2D gel
86 evidence in the above initial reports suggests that this was not the case.

87 To clarify the Tof1-Csm3 relationship with Rrm3 we utilized several replication fork pausing and
88 instability assays (**Fig. 1**). Deletion of *TOF1* or *CSM3* led to a strong decrease in paused fork signal at Fob1-
89 RFB detected by 1D gels, as expected (**Fig. 1C**). Significantly, *tof1Δ* mutation also decreased fork pausing in a
90 *rrm3Δ* background (**Fig. 1B, 1C**), suggesting that in cells lacking Rrm3 helicase, Tof1 still actively promotes
91 replication fork slowdown (**Fig. 1A, model '2'**). Next, we used chromatin immunoprecipitation to probe
92 binding of the replicative helicase components Mcm4 and Cdc45, as it was reported that replisome
93 components are more enriched at pause sites (Azvolinsky et al. 2009). Consistent with the 1D and 2D gel
94 analysis, we detected Tof1-dependent enrichment of Mcm4 and Cdc45 on several pause sites in cells lacking
95 Rrm3 helicase (**Fig. 1D and S1D**), while pausing at telomeres was less dependent on Tof1.

96 Lack of the Rrm3 helicase leads to prolonged fork pausing at Fob1-RFB and elevated rDNA instability
97 as a result of fork pausing (Ivessa et al. 2000). Utilizing *ADE2* marker loss from the rDNA locus as a measure
98 of ribosomal gene array instability, we found that Tof1 was required for rDNA repeat destabilization in *rrm3Δ*
99 cells (**Fig. 1E**). Remarkably, *tof1Δ* mutation also suppressed the more elevated instability of an *rrm3Δ rif1Δ*
100 double mutant, which additionally lacks a negative regulator of replication origin firing, Rif1 (Shyian et al.
101 2016). Viability of *rif1Δ* cells requires the DSB repair and fork maintenance complex MRX, and the lethality
102 caused by MRX mutations in these cells is suppressed by pausing alleviation through *fob1Δ*, *tof1Δ*, or *csm3Δ*
103 mutations (Shyian et al. 2016). Notably, we observed that *tof1Δ* partially suppressed synthetic sickness of
104 *rrm3Δ* and *mre11Δ* mutations, to an extent slightly stronger than suppression by *fob1Δ* (**Fig. 1F**). This
105 difference in suppression by *tof1Δ* compared to *fob1Δ* is perhaps related to a more general role of Tof1 in
106 replisome pausing throughout the genome, since Fob1 is thought to act exclusively at rDNA repeats.
107 Altogether, our results show that Tof1 mediates fork pausing, rDNA instability and cellular toxicity in cells
108 lacking Rrm3 helicase. Therefore, it is unlikely that Tof1 promotes fork pausing exclusively by regulating
109 Rrm3 helicase but rather suggests a more direct involvement of Tof1-Csm3 in fork slowdown (**Fig. 1A**, model
110 '2'), albeit through an unknown mechanism.

111 ***Tof1-Csm3 complex interacts with Top1***

112 Intrigued by the strong rDNA stabilizing effect of *tof1Δ* mutation (**Fig. 1E**), we sought to identify the
113 factor(s) contributing to this stability and regulating replication fork pausing at Fob1-RFB. We carried out an
114 unbiased forward genetic screen for mutants de-stabilizing the rDNA in either a wild type (WT) or *tof1Δ*
115 background, using *ADE2* and *URA3* loss from the array as a read-out (the “cowcatcher” screen, Materials and
116 Methods; **Fig. S2A**). Mutations in *RRM3*, *SIR2*, *HST3*, *CAC1*, *ORC1* and *PSF2* genes were recovered in the WT
117 background but not in *tof1Δ*. One of the mutations we discovered specifically in the *tof1Δ* background was in

118 the *TOP1* gene, which encodes topoisomerase I (**Fig. S2A**) – an enzyme required for both DNA replication and
119 stability of rDNA repeats (Christman et al. 1988; Kim and Wang 1989b; Kim and Wang 1989a). The highly
120 negative score of this *top1-G297D* mutation in Protein Variation Effect Analyzer (Choi et al. 2012) (PROVEAN:
121 -7; cutoff = -2.5) implied a deleterious effect of this change on Top1 function. Indeed, complete deletion of
122 the *TOP1* ORF led to a strong elevation of rDNA instability (**Fig. 2A**). In contrast to *rrm3Δ* and *rif1Δ* mutations
123 however, the rDNA instability in *top1Δ* cells was not suppressed by *tof1Δ*, suggesting that Top1 and Tof1 may
124 have overlapping roles. This and the fact that *TOF1* was originally identified in a yeast two-hybrid screen that
125 employed a part of Top1 protein as a bait, as its name implies ('TOpoisomerase I-interacting Factor 1'; (Park
126 and Sternglanz 1999)), prompted us to focus further on this factor.

127 As mentioned above, Tof1-Csm3 is present in the cell nucleus within the MTC complex, together with
128 Mrc1 (Bando et al. 2009). Using co-immunoprecipitation experiments, we observed that topoisomerase I
129 was indeed recovered together with all the three components of the MTC complex (**Fig. 2B, S2B**). This
130 interaction was detected only when whole cell extracts were treated with Benzonase nuclease, which
131 degrades nucleic acids and liberates protein complexes from chromatin (De Piccoli et al. 2012) (**Fig. S2C**).
132 Importantly, the MTC-Top1 interaction depended only on Tof1 and Csm3 proteins, but not Mrc1 (**Fig. 2B,**
133 **S2B**), suggesting that Mrc1 interacts with Top1 indirectly through a Tof1-Csm3 sub-complex.

134 ***Tof1-Csm3 promotes Top1 recruitment to the replisome***

135 Since both Tof1-Csm3 and Top1 are components of the RPC (Gambus et al. 2006) we wondered
136 whether the interaction of Tof1-Csm3 with Top1 occurs in the context of the replisome, which might explain
137 how Top1 is recruited to the replication fork. To investigate this possibility, we conducted chromatin
138 immunoprecipitation (ChIP) experiments to assess Top1 recruitment to origins of replication in cell cultures
139 synchronously released into S phase from α -factor induced G1 arrest. We detected Top1 association with

140 early origins (*ARS305* and *ARS607*) at the time of their activation (**Fig. 2C** and **S2D**) in accordance with a
141 previous study (Bermejo et al. 2007). However, cells lacking Tof1 had much lower levels of Top1 recruitment
142 to these (**Fig. 2C** and **S2D**). To confirm this result, we analyzed the genome wide binding of Top1 in early S
143 phase and observed, as expected, that Top1 is enriched at replicating ARSs (**Fig. 2D**) and highly transcribed
144 genes (**Fig. S2E**) that correspond to regions experiencing high helical tension. Remarkably, removing Tof1
145 abolished the Top1 signal at ARSs, whereas binding at promoters of highly transcribed genes was not
146 affected. Furthermore, absence of the MTC complex member Mrc1 did not affect Top1 recruitment (**Fig. 2C**
147 and **S2D**), which is in line with retention of the Tof1-Top1 interaction in *mrc1Δ* cells (**Fig. 2B** and **S2B**).
148 Moreover, absence of the Rrm3 helicase did not restore the Top1 association with origins in *tof1Δ* cells (**Fig.**
149 **2C** and **S2D**).

150 The last 258 amino acid residues of the C-terminal part of Tof1 were reported to be sufficient for the
151 two-hybrid interaction with Top1 (Park and Sternglanz 1999). Consistent with this part of Tof1 harboring a
152 Top1-interacting domain, we observed a loss of Top1 co-immunoprecipitation and recruitment to origins in
153 cells expressing a Tof1 protein lacking the last 258 aa (*tof1-ΔC* = *tof1-Δ⁹⁸¹⁻¹²³⁸-3xFLAG*) (**Fig. 2E-F** and **S2F-G**).
154 Importantly, recruitment of WT Tof1 and the truncated Tof1-ΔC protein to origins was comparable (**Fig. 2F**
155 and **S2F-G**). This suggests that Tof1 promotes Top1 association with origins by directly recruiting Top1 to the
156 replisome.

157 ***Top1 positively regulates replication fork pausing at RFBs***

158 As it is not understood how Tof1-Csm3 slows down the replication fork at protein barriers, we
159 wondered if their interactor Top1 is involved in this process. In order to assess this putative functional link
160 between Tof1 and topoisomerase I, we evaluated replication pausing at RFBs in asynchronous cultures.
161 Indeed, deletion of *TOP1* or dissociation of Top1 from the replisome by *tof1-ΔC* mutation led to a similar ca.

162 50% decrease in pausing at RFBs both in WT and *rrm3Δ* backgrounds, as detected by 2D and 1D gels at rRFB
163 (**Fig. 3A** and **S3A-B**) or by Mcm4-MYC CHIP at rRFB and tRNA genes (**Fig. 3B** and **S3C**). Moreover, the fork
164 pausing decrease in the double mutant *tof1-ΔC top1Δ* was comparable to that of single *tof1-ΔC* and *top1Δ*
165 mutants (**Fig. 3B**), suggesting that the two factors could act in the same pausing pathway. Consistent with
166 retention of Top1 recruitment to the FPC complex and to the replisome, *mrc1Δ* had no defect in pausing (**Fig.**
167 **S3B**), as previously shown (Tourriere et al. 2005; Hodgson et al. 2007). Moreover, as the *mrc1Δ* mutation is
168 known to decrease fork progression rates even more strongly than does *tof1Δ*, but has no effect on pausing
169 (Tourriere et al. 2005; Hodgson et al. 2007), it seems unlikely that the decreased fork pausing in *tof1-ΔC* or
170 *top1Δ* mutant could be an indirect consequence of any potential change in fork progression rates in these
171 mutants.

172 We had shown previously (Shyian et al. 2016) that *rif1Δ* leads to increased initiation at the rDNA ARS
173 elements. One consequence of this is increased fork stalling and collapse at the rRFB, which leads to
174 synthetic sickness in combination with *mre11Δ*. This synthetic growth defect is abolished by deletion of
175 *FOB1*, confirming its connection to the rDNA fork block. As expected for a pausing defect, we found that
176 *tof1-ΔC* partially alleviated *rif1Δ mre11Δ* synthetic sickness (**Fig. 3C**).

177 The fact that cells lacking Top1 completely or lacking the Top1-recruiting C-terminus of Top1 still
178 exhibit a pause signal significantly higher than cells lacking the whole of Top1 protein (**Fig. 3A**) suggests that
179 some other factor(s) are able to compensate for Top1 loss in a Top1-dependent way and slow down the
180 replisome in the absence of Top1.

181 ***Top1 and Top2 redundantly promote fork pausing at Fob1-RFB***

182 Top1 is believed to be the main replicative swivelase (Kim and Wang 1989a), but it is not essential for
183 replication elongation and survival in budding yeast since Top2 is able to compensate for its absence (Kim
184 and Wang 1989a; Bermejo et al. 2007). Consistent with this, we also detected Top2 in the
185 immunoprecipitates of Top1 and Csm3 proteins (**Fig. S4A**) and *tof1-ΔC* mutation only partially affected this
186 association (**Fig. S4B**). We asked then whether Top2 could compensate for the loss of the Top1 in the
187 replication fork pausing. Indeed, while inactivation of topoisomerase II at elevated temperature in a *top2-ts*
188 strain or by auxin-induced degradation of the protein had only a little effect on pausing (**Fig. 4A-B** and **S4C-D**)
189 doing so in cells lacking Top1 (*top1Δ*) or in cells with Top1 destabilized from the replisome (*tof1-ΔC*) led to a
190 dramatic fork pausing loss phenotype similar to the one in *tof1Δ* cells (**Fig. 4A-B, S4C-D** and **S4F-G**).

191 We observed a similar loss of fork slowdown when using different means to simultaneously deplete
192 Top1 and Top2: temperature inactivation of Top2 in *top1Δ top2-ts* and *tof1-ΔC top2-ts* strains (**Fig. 4A-B** and
193 **S4C**), degradation of both proteins (Top1-AID and Top2-AID) or degradation of Top2 in *top1Δ* and/or *tof1-ΔC*
194 cells by the auxin-induced degron (Morawska and Ulrich 2013) system (**Fig. S4D-G**) and anchoring away
195 (Haruki et al. 2008) of Top2 in a *top1Δ TOP2-FRB* background (**Fig. S4H**). Depletion of Top3 on its own or in
196 combination with either Top1 or Top2 did not abolish the block (**Fig. S4D**), in accord with a recent study
197 (Mundbjerg et al. 2015) and consistent with Top3 having a role in recombination but not replication
198 (Pommier et al. 2016). Remarkably, replication intermediates in cells lacking both Top1 and Top2 had an
199 appearance very similar to those of *tof1Δ* strains (**Fig. 3A, 4A**, and **S4C-H**), in which the loss of the pausing
200 signal at the Fob1-RFB was accompanied by an increase in the intensity of the descending part (left half) of
201 the Y arc. We speculate that the latter might be due to a head-on collision of the replication fork liberated
202 from Fob1-RFB with the RNA polymerase I transcribing the adjacent rRNA gene. Thus, Top1 and Top2

203 proteins act in parallel to promote replication fork pausing at Fob1-RFB, and the replisome appears to be able
204 to move past the Fob1-RFB in their absence.

205 Nevertheless, these data have to be interpreted with caution since it was reported that simultaneous
206 inactivation of topoisomerase I and II leads to DNA damage checkpoint activation and to rapid replication
207 cessation (Bermejo et al. 2007), which could in theory contribute to the observed fork pausing phenotypes.
208 However, addressing the checkpoint issue, we found that degradation of both Top1 and Top2 in the
209 checkpoint-deficient backgrounds *rad53-K227A* (kinase-dead Rad53) or *rad9Δ* abolished pausing to an extent
210 similar to that in checkpoint-proficient cells (**Fig. S4H**), indicating that checkpoint activation is not necessary
211 for the loss of replication fork slowdown. With regard to replication cessation, when released from G1 arrest
212 into S phase at +37 °C, *top1Δ top2-ts* strains indeed failed to progress through S phase and arrested with
213 close to 1C DNA content (**Fig. 4C**), consistent with previous findings (Kim and Wang 1989a; Bermejo et al.
214 2007). However, *tof1-ΔC top2-ts* and *tof1Δ top2-ts* cells rapidly progressed through the S phase in these
215 conditions (similarly to *top2-ts* only cells (**Fig. 4C and S4E**)). Since both *top1Δ top2-ts* and *tof1-ΔC top2-ts*
216 cells show a similar decrease of fork pausing at +37 °C (**Fig. 4A-B, S4C-D**), while only the former exhibits an S
217 phase progression defect, we reasoned that the fork slowdown by Top1 and Top2 is not an indirect
218 consequence of their genome-wide replication role but rather an *in cis* effect of these topoisomerases at the
219 replisome, promoted by the Tof1-Csm3 complex. Moreover, it appears that Top1 (and perhaps Top2)
220 anchoring at the replisome by Tof1 is not essential for the general S phase progression but is specifically
221 important for fork pausing.

222 ***tof1-ΔC is a separation of function mutation that leaves replication checkpoint roles intact***

223 Since Tof1-Csm3 is an evolutionary conserved complex performing both fork pausing and replication
224 checkpoint functions at the replisome (McFarlane et al. 2010), we wondered if the Tof1 C-terminus might be
225 specifically involved in only the fork pausing role.

226 First, similar to the wild-type version, Tof1-ΔC protein appears to protect its partner Csm3 from
227 degradation (**Fig. 5A**), an evolutionarily-conserved Tof1 function (Chou and Elledge 2006; Bando et al. 2009).
228 Next, Tof1 positively regulates the DNA replication checkpoint (DRC) (Foss 2001), promoting survival of DNA
229 damage response-deficient cells (*rad9Δ*) subjected to hydroxyurea-induced replication stress. Tof1-ΔC was
230 still able to carry out this function (**Fig. 5B**), indicating that it is likely checkpoint-proficient. Accordingly, Tof1-
231 ΔC supported DRC activation as measured by Rad53 phosphorylation in both *rad9Δ* and in WT cells (**Fig. 5C**
232 and **5B**), while *tof1Δ rad9Δ* cells had a prominent defect in Rad53 phosphorylation similar to checkpoint
233 defective *mec1Δ sml1Δ* cells, as expected (Foss 2001). Furthermore, Tof1 and Mrc1 appear to act in the same
234 DRC pathway, as *tof1Δ* and *tof1Δ mrc1Δ* cells showed a similar defect in Rad53 phosphorylation under HU
235 treatment (**Fig. 5D**), consistent with known role of the Tof1 in promoting Mrc1 association with replication
236 forks (Bando et al. 2009).

237 The loss of Tof1-Csm3 complex, but not Mrc1, confers strong sensitivity to the Top1-trapping agent
238 camptothecin (CPT) (Redon et al. 2006; Reid et al. 2011) (**Fig. 5E** and **S5A-B**). We found in addition that cells
239 lacking any of the MTC complex components display impaired growth in the presence of etoposide (ETOP)
240 (**Fig. 5E** and **S5A-B**), a chemical blocking topoisomerase II, with *tof1Δ* and *csm3Δ* again having a greater effect
241 than *mrc1Δ*. Importantly, *tof1Δ* and *csm3Δ* mutations impaired growth specifically in the presence of
242 topoisomerase blocking agents but not upon DNA double-strand break induction by phleomycin or fork
243 stalling and breakage by the alkylating agent MMS (**Fig. S5A-B**). Therefore, the Tof1-Csm3 complex appears

244 to protect cells from blocked topoisomerases. We wondered whether this protection stems from the ability
245 of Tof1-Csm3 to engage with Top1 and Top2. Surprisingly, *tof1-ΔC* mutant was still significantly resistant to
246 CPT and ETOP (**Fig. 5E**). We reasoned that the higher sensitivity of *tof1Δ* to these agents in contrast to *tof1-*
247 *ΔC* mutant could be due to the preservation of another function in the Tof1-ΔC protein and, since Tof1-ΔC is
248 proficient in the Mrc1-dependent DRC (**Fig. 5C** and **4D**), speculated that this might also be related to a role
249 shared with Mrc1. We therefore removed Mrc1 from the *tof1-ΔC* mutant cells and indeed observed an
250 increase in CPT and ETOP sensitivity in the *tof1-ΔC mrc1Δ* double mutant, to an extent comparable to that of
251 *tof1Δ* cells (**Fig. 5E**). Interestingly, *tof1Δ*, but not *tof1-ΔC*, grew slowly in combination with *mrc1Δ* (at 25°C;
252 **Fig. 5E**) and in spore colonies, suggesting that Tof1-ΔC protein still performs an additional function important
253 for growth in parallel to Mrc1. Thus, the Tof1-Csm3 complex appears to protect the cell from trapped
254 topoisomerases by both interacting with them directly (through the C-terminus of Tof1, and perhaps other
255 regions) and by acting together with Mrc1, likely by promoting the DRC and/or stabilizing forks at the
256 topoisomerase-trapping sites (Strumberg et al. 2000).

257 **DISCUSSION**

258 In summary, we showed that Tof1-Csm3 mediates replication fork pausing at proteinaceous RFBs
259 through a pathway independent of Rrm3 helicase. Instead, Tof1-Csm3 complex interacts with
260 topoisomerases I and II and mediates Top1 association with the replisome in normal S phase. Although we
261 did not detect Top2 recruitment to replisomes in unchallenged cells with ChIP, alternative approaches should
262 be used in the future to assess Top2 recruitment and its dependency on FPC. Top1 was previously identified
263 as a part of the RPC (Gambus et al. 2006) and our report pinpoints the precise factor responsible for its
264 engagement and suggests that eukaryotic cells do not rely exclusively on the DNA topology-mediated
265 recruitment of topoisomerases to replicate chromosomes but rather have an association hub (Tof1-Csm3) to
266 enrich them on the replisome. We imagine that this pathway could serve to prevent buildup of excess

267 torsional stress in the vicinity of the replisome, by ensuring topoisomerase presence. This may avert
268 uncontrolled escape of supercoils away from the fork by diffusion, supercoil ‘hopping’ (van Loenhout et al.
269 2012) or fork rotation (Schalbetter et al. 2015), possibilities that warrant further investigation.

270 Our findings indicate that either Top1 or Top2 is able to impose replication fork pausing at the Fob1-
271 RFB, through a mechanism that we dub ‘sTOP’ (‘slowing down with TOPoisomerase I and II’) (**Fig. 6**). Indeed,
272 it is assumed that in eukaryotes topoisomerase I and II act in front of the replication fork to unlink the
273 parental DNA strands (Brill et al. 1987; Duguet 1997), while topoisomerase II acts also behind the fork to
274 remove precatenanes. Either Top1 or Top2 is sufficient to assist in DNA replication elongation (Pommier et
275 al. 2016), explaining why *TOP1* is not essential. The essential role of *TOP2* stems not from the replication
276 elongation step, but from its crucial role in chromosome segregation during replication termination (Baxter
277 and Diffley 2008). We imagine that the local increase in topoisomerase concentration/activity in the vicinity
278 of replisome afforded by Tof1-Csm3 recruitment might assist general replication elongation by alleviating
279 torsional stress. In cells lacking the Tof1-Csm3 complex topoisomerases would act more distributively but
280 still ensure replisome progression, albeit perhaps less efficiently. We note that recruitment of an essential
281 enzymatic function to the replisome by non-essential RPC factors is not unprecedented, since another RPC
282 component, Ctf4, serves to recruit DNA polymerase α /primase (Simon et al. 2014) and Mrc1 stimulates the
283 interaction of the leading strand DNA polymerase ϵ (Lou et al. 2008).

284 In order to assist in DNA replication, the topoisomerase swivelase should be placed in front of the
285 replication fork (Duguet 1997) – a setting where Top1 and Top2 might be the first replisome components to
286 encounter obstacles. The slowing of the replication fork could be either a consequence of an inhibitory signal
287 propagating from stalled topoisomerases through Tof1-Csm3 to the CMG helicase, or a result of
288 topoisomerase activity itself. Consistent with first mode of action, it was reported that Tof1-Csm3
289 orthologues are able to inhibit the ATPase activity of MCM proteins *in vitro* (Cho et al. 2013). According to

290 the second model, the absence of Top1 and Top2 at the replisome might promote bypass of barriers by
291 increasing superhelical tension at the fork and simplifying blocking protein dissociation from DNA. In line
292 with this possibility, bacterial *topA* mutants cause a loss of replication fork pausing at Tus/Ter sites likely by
293 an increase in negative superhelicity, as this is suppressed by compensatory *gyrB* mutations (Valjavec-Gratian
294 et al. 2005). Moreover, it was proposed that topoisomerase inhibition leads to nucleosome destabilization
295 due to increased positive torsion ahead of transcribing RNA polymerase II (Teves and Henikoff 2014). It is
296 thus tempting to speculate that by recruiting topoisomerases to the fork, Tof1-Csm3 precludes torsional
297 stress buildup ahead of the replisome, helping to maintain integrity of chromatin (binding of both non-
298 histone and histone proteins). Further studies, particularly with single-molecule approaches, will help to
299 assess whether this is the case and elucidate the exact molecular details of how Top1 and Top2 promote the
300 replication fork pausing at proteinaceous barriers and general fork progression.

301 Although topoisomerase would still be expected to assist DNA elongation by replisomes lacking the
302 Tof1-Csm3 complex (since *tof1Δ* and *csm3Δ* cells are viable), the failure to recognize topoisomerases in front
303 of the fork, and perhaps to duly pause until they dissociate from the template, might lead to replisome-
304 topoisomerase collisions. We speculate that collision and replication run-off (Strumberg et al. 2000) with
305 subsequent failure to properly activate checkpoint and repair the collapsed forks might explain the elevated
306 sensitivity of *tof1Δ* and *csm3Δ* mutants to topoisomerase blocking conditions (**Fig. 5D, S5A-B**) (Redon et al.
307 2006; Reid et al. 2011). Accordingly, it was recently proposed that the Csm3 orthologue TIPIN may help to
308 recognize topoisomerase I trapped by CPT and preclude replisome collision with it (Hosono et al. 2014).

309 This novel replication fork ‘STOP’ mechanism offers a solution to an unresolved problem of how
310 Tof1-Csm3 manages to recognize molecularly distinct RFBs: the Top1 and Top2 topological (or physical)
311 interaction with RFBs might serve as a unifying common feature of different barriers. We also note that
312 catalytically engaged Top1 is present at the Fob1-RFB (due to an interaction with Tof2 (Krawczyk et al. 2014))

313 throughout the cell cycle (Di Felice et al. 2005) and Top1 assists in progression of RNA polymerase II
314 complexes (Teves and Henikoff 2014; Baranello et al. 2016). Therefore, an intriguing question would be
315 whether Tof1-Csm3 could mediate recognition by the replisome of Top1 and Top2 present as a part of these
316 and other chromatin complexes in the path of a replication fork.

317 Recently DNA replication elongation reactions (Yeeles et al. 2017) and fork pausing at Fob1 barriers
318 were successfully reconstituted *in vitro* (Hizume et al. 2018), where Tof1-Csm3 supported high elongation
319 rates and mediated pausing. It will be of interest to test whether these *in vitro* phenotypes of Tof1-Csm3 are
320 mediated via recruitment of Top1 and Top2 to the replisome. Another fascinating question is whether the
321 role of Tof1-Csm3 orthologues in other systems, such as replication pausing and imprinting control by Swi1-
322 Swi3 at the *mat* locus in fission yeast (Dalgaard and Klar 2000), circadian clock regulation in metazoans
323 (McFarlane et al. 2010), and survival in the face of replication stress (Bianco et al. 2019) are mediated via
324 interactions with topoisomerases.

325

326 **Materials and Methods**

327 ***Yeast strains, genetics and growth conditions***

328 Standard genetic methods for budding yeast strain construction and crossing were used (Shyian et al. 2016).
329 Strains used in this study are listed in the **Table S1**. Genotoxic agent sensitivity was assessed in multidrug-
330 sensitive yeast background (Chinen et al. 2011). For growth assays, saturated cultures of the respective
331 genotypes were serially diluted (1:10) and spotted onto YPAD plates or YPAD plates supplemented with
332 genotoxic agents. The plates were imaged following 2-4 days of incubation at 30°C or 25°C. *ADE2* marker
333 loss assays were performed essentially as in (Shyian et al. 2016). Degradation of AID-tagged proteins

334 (Morawska and Ulrich 2013) and cytoplasmic anchoring of the FRB-tagged proteins (Haruki et al. 2008) was
335 achieved by addition of 1 mM IAA (Indole-3-acetic acid) or 1 mkg/mL RAPA (Rapamycin) for 60 minutes to
336 the exponentially growing cultures. Heat inactivation of the Top2-ts protein was achieved by shifting
337 exponentially growing yeast cultures from +25°C to +37°C for 60 minutes. For the cell cycle progression
338 analysis in *top2-ts* background, the exponentially growing cells were arrested in G1 with α F treatment at
339 +25°C during 2.5 hrs, transferred to +37°C for an additional 1 hr, washed 2x times with H₂O, and released
340 from the G1 arrest at +37°C in pronase-containing medium (Mattarocci et al. 2014).

341 ***rDNA instability (ADE2 loss) assay***

342 rDNA instability was assessed by the *ADE2* marker loss assay (Kaeberlein et al. 1999; Shyian et al. 2016).
343 Saturated yeast cultures were diluted in water to around 400 cells per volume and plated onto YPD plates
344 supplemented with 5 mg/ml adenine or onto SC plates (with or without 5-FOA). Plates were incubated at
345 30°C for 3 days, then at 4°C during 2 days and subsequently at 25°C for 1 day. The colonies were counted
346 using ImageJ software Colony Counter plugin and the marker loss was plotted as the percentage of white
347 colonies having red sectors to all the colonies except completely red colonies (where *ADE2* marker was lost in
348 previous cell divisions).

349 ***1D and 2D gels and Southern blot***

350 2D gels were performed essentially as in (Shyian et al. 2016) using BglII enzyme for genomic DNA digestion
351 and Fob1-RFB Southern blot hybridization probe. The images were acquired with Typhoon FLA 9500 (GE
352 Healthcare Life Sciences) and the intensity of signals quantified with ImageQuant TL 8.1 Software (GE
353 Healthcare Life Sciences). The ratio of the signals at the rRFB spot to the remainder of Y arc of a given
354 mutant was normalized to the respective ratio in WT present on the same 2D gel membrane and reported as

355 'Replication forks at RFB relative to *Y arc*' value; this value in all the WT samples therefore equals 1. For 1D
356 gels the first dimension gel was stained with EtBr, directly transferred to nylon membrane and probed with a
357 radioactively labeled probe specific to Fob1-RFB site (Brewer and Fangman 1988; Kobayashi et al. 2004). The
358 membranes were exposed to K-screens (Bio-Rad) for 6 hrs to 7 days before phosphorimaging.

359 **Chromatin Immunoprecipitation (ChIP)**

360 Mcm4-13MYC, Cdc45-13MYC, Top1-13MYC anti-Myc and Tof1-3FLAG, Tof1-980aa-3FLAG anti-FLAG ChIP
361 assays were performed essentially as in (Mattarocci et al. 2014). Mcm4-13MYC and Cdc45-13MYC ChIP
362 experiments were done using asynchronously growing cultures. Where indicated, precipitated DNA was used
363 to prepare sequencing libraries with TruSeq (illumine) and sequenced on iGE3 Genomics Platform of
364 University of Geneva. FASTQ files were mapped to *S. cerevisiae* genome with Mapping tool of 'HTSstation'
365 (David et al. 2014). Cell synchronization and flow cytometry assays were performed essentially as described
366 in (Mattarocci et al. 2014).

367 **'Cowcatcher' screen**

368 Strains containing single copy of *ADE2* and *URA3* genes inserted into rDNA array were used for mutagenesis
369 with EMS at 50% survival. EMS-treated cultures were split in 10 separate tubes, inoculated into SC-ADE-URA
370 liquid medium and grown overnight (to counter-select mutations in *ADE2* and *URA3*). Then, aliquots were
371 inoculated into YPAD and grown overnight to allow for marker loss from the rDNA. Dilutions were plated on
372 5-FOA plates (selection for *URA3* loss) and incubated as in *ADE2* loss assay above. After visual inspection, red
373 sectorized colonies from 5-FOA plates were manually selected and their white sectors were streaked
374 sequentially 2 times onto SC plates. Of ca. 50'000 colonies from 5-FOA plates, 30 independent, reproducibly
375 high-sectoring isolates were chosen. These were back-crossed, sporulated, dissected and assessed for

376 segregation of the high sectoring phenotype. Isolates showing 2:2 segregation for sectoring (consistent with
377 Mendelian mono-allelic mutations) were subjected to causative mutation identification using Pooled Linkage
378 Analysis (as in (Birkeland et al. 2010; Lang et al. 2015)). Briefly, 20 spore colonies with a sectoring phenotype
379 were pooled (+phenotype) and 20 white spore colonies were pooled (-phenotype) and their genomic DNA
380 was isolated with a Qiagen genomic tip kit. Total genomic DNA of the two pools was submitted to iGE3
381 Genomics Platform of University of Geneva for fragmentation, library preparation and whole genome deep
382 sequencing. The resulting FASTQ files were mapped to *S. cerevisiae* genome with Mapping tool of
383 'HTSstation' (David et al. 2014). The SNPs were identified with the SNP tool of 'HTSstation'. The SNPs
384 unique/over-represented in the plus-phenotype pool compared to the minus-phenotype pool were identified
385 in Excel.

386 ***Co-immunoprecipitation, SDS-PAGE and Western blot***

387 Co-immunoprecipitation was performed as in (Gambus et al. 2006) and (De Piccoli et al. 2012). Briefly, 50 mL
388 of exponentially growing cells at $OD_{600} = 0.6$ were pelleted, washed 2x times with cold H_2O , suspended in 1
389 mL of Lysis Buffer (100 mM HEPES-KOH pH 7.9, 100 mM potassium acetate, 10 mM magnesium acetate, 10%
390 glycerol, 0.1% NP-40, 2 mM EDTA, 2 mM glycerol 2-phosphate, and freshly added: 2 mM sodium fluoride, 1
391 mM DTT, 1 mM PMSF, Roche Protease Inhibitor Cocktail and PhosStop) and transferred into a cryotube with
392 500 μ L of Zirconia/silica beads. The cells were homogenized in a Minibeadbeater at max power 2x times for
393 1.5 min with a 1 min interval. The lysed cells were recovered by centrifugation through a hole in the bottom
394 of a cryotube and treated with 100 U of Benzonase (Millipore) for 40 min at $+4^\circ C$ with rotation. The whole-
395 cell extract (WCE) was obtained as supernatant after centrifugation at 13000 rpm for 30 min at $+4^\circ C$. 30 μ L
396 of IgG Sepharose beads pre-washed 4x times with Lysis Buffer were used for immunoprecipitation of the TAP-
397 tagged proteins from the WCE during 2 hrs at $+4^\circ C$ with rotation. The beads were washed 3x times with Lysis

398 Buffer at +4°C with rotation and boiled for 10 min with 50 μ L of 2x Laemmli Buffer. The proteins were
399 resolved on 8% iD PAGE GELS (Eurogentec), transferred onto nitrocellulose membrane (Amersham). The
400 proteins were detected with anti-TAP (ThermoFisher), anti-MYC (Cell Singaling) or anti-FLAG (Sigma)
401 antibodies. For Csm3-TAP protein level detection (Fig. 4A) and for Rad53 phosphorylation detection (Fig. 4C
402 and 4D) total cellular proteins were isolated using TCA-Urea method (Mattarocci et al. 2014). Total and
403 active auto-phosphorylated Rad53 were detected with Rad53 protein antibodies (Mab clone EL7) and (Mab
404 clone F9) respectively provided by A. Pellicoli (University of Milan) (Fiorani et al. 2008).

405 ***Statistical methods***

406 Welch's t test (two-tailed, unpaired t test with Welch's correction) was used to assess statistical significance
407 of differences in all the quantitative comparisons (* $p < 0.05$; ** $p < 0.01$; *** $p < 0.001$; **** $p < 0.0001$). Mean
408 values \pm SEM (standard error of the mean) are reported on graphs. GraphPad Prism 8 (GraphPad Software,
409 Inc) was used to prepare the graphs and perform statistical comparisons.

410

411 **Acknowledgements**

412 We thank Nataliia Serbyn for discussions, advice and assistance; Jessica Bruzzone for assistance with
413 sequencing library preparation, Slawomir Kubik for advice on data analysis and all members of Shore Lab for
414 critical comments. We thank iGE3 Genomics Platform of the University of Geneva for sequencing library
415 preparation and high-throughput sequencing experiments. We thank Benoit Kornmann for the advice on the
416 Pooled Linkage Analysis; Usui Takeo for sharing 12gene Δ OHSR background strains and Francoise Stutz for the
417 BY deletion and DAMP strains. We thank Nicolas Roggli for expert graphical work; Pascal Damay for ordering
418 and maintaining reagent stocks.

419

420 **Author contributions**

421 MS conceived the project. MS, BA and DS designed all the experiments. MS, BA, AMZ, VI, GC and DD
422 performed the experiments and analyzed the data. BA and VI contributed strains and reagents. MS wrote
423 the manuscript, which was revised by MS and DS with input from BA.

424 **Declaration of Interests**

425 The authors declare no competing interests.

426

427 **REFERENCES**

428

- 429 Azvolinsky A, Dunaway S, Torres JZ, Bessler JB, Zakian VA. 2006. The *S. cerevisiae* Rrm3p DNA helicase
430 moves with the replication fork and affects replication of all yeast chromosomes. *Genes Dev* **20**:
431 3104-3116.
- 432 Azvolinsky A, Giresi PG, Lieb JD, Zakian VA. 2009. Highly transcribed RNA polymerase II genes are
433 impediments to replication fork progression in *Saccharomyces cerevisiae*. *Mol Cell* **34**: 722-734.
- 434 Bairwa NK, Mohanty BK, Stamenova R, Curcio MJ, Bastia D. 2011. The intra-S phase checkpoint protein
435 Tof1 collaborates with the helicase Rrm3 and the F-box protein Dia2 to maintain genome
436 stability in *Saccharomyces cerevisiae*. *J Biol Chem* **286**: 2445-2454.
- 437 Bando M, Katou Y, Komata M, Tanaka H, Itoh T, Sutani T, Shirahige K. 2009. Csm3, Tof1, and Mrc1 form a
438 heterotrimeric mediator complex that associates with DNA replication forks. *J Biol Chem* **284**:
439 34355-34365.
- 440 Baranello L, Wojtowicz D, Cui K, Devaiah BN, Chung HJ, Chan-Salis KY, Guha R, Wilson K, Zhang X, Zhang
441 H et al. 2016. RNA Polymerase II Regulates Topoisomerase 1 Activity to Favor Efficient
442 Transcription. *Cell* **165**: 357-371.
- 443 Baxter J, Diffley JF. 2008. Topoisomerase II inactivation prevents the completion of DNA replication in
444 budding yeast. *Mol Cell* **30**: 790-802.
- 445 Bell SP, Labib K. 2016. Chromosome Duplication in *Saccharomyces cerevisiae*. *Genetics* **203**: 1027-1067.

- 446 Bermejo R, Dokhani Y, Capra T, Katou YM, Tanaka H, Shirahige K, Foiani M. 2007. Top1- and Top2-
447 mediated topological transitions at replication forks ensure fork progression and stability and
448 prevent DNA damage checkpoint activation. *Genes Dev* **21**: 1921-1936.
- 449 Bianco JN, Bergoglio V, Lin YL, Pillaire MJ, Schmitz AL, Gilhodes J, Lusque A, Mazieres J, Lacroix-Triki M,
450 Roumeliotis TI et al. 2019. Overexpression of Claspin and Timeless protects cancer cells from
451 replication stress in a checkpoint-independent manner. *Nature Communications* **10**.
- 452 Birkeland SR, Jin N, Ozdemir AC, Lyons RH, Jr., Weisman LS, Wilson TE. 2010. Discovery of mutations in
453 *Saccharomyces cerevisiae* by pooled linkage analysis and whole-genome sequencing. *Genetics*
454 **186**: 1127-1137.
- 455 Brewer BJ, Fangman WL. 1988. A replication fork barrier at the 3' end of yeast ribosomal RNA genes. *Cell*
456 **55**: 637-643.
- 457 Brill SJ, DiNardo S, Voelkel-Meiman K, Sternglanz R. 1987. Need for DNA topoisomerase activity as a
458 swivel for DNA replication for transcription of ribosomal RNA. *Nature* **326**: 414-416.
- 459 Chinen T, Ota Y, Nagumo Y, Masumoto H, Usui T. 2011. Construction of multidrug-sensitive yeast with
460 high sporulation efficiency. *Biosci Biotechnol Biochem* **75**: 1588-1593.
- 461 Cho WH, Kang YH, An YY, Tappin I, Hurwitz J, Lee JK. 2013. Human Tim-Tipin complex affects the
462 biochemical properties of the replicative DNA helicase and DNA polymerases. *Proc Natl Acad Sci*
463 *U S A* **110**: 2523-2527.
- 464 Choi Y, Sims GE, Murphy S, Miller JR, Chan AP. 2012. Predicting the functional effect of amino acid
465 substitutions and indels. *PLoS One* **7**: e46688.
- 466 Chou DM, Elledge SJ. 2006. Tipin and Timeless form a mutually protective complex required for
467 genotoxic stress resistance and checkpoint function. *Proc Natl Acad Sci U S A* **103**: 18143-18147.
- 468 Christman MF, Dietrich FS, Fink GR. 1988. Mitotic recombination in the rDNA of *S. cerevisiae* is
469 suppressed by the combined action of DNA topoisomerases I and II. *Cell* **55**: 413-425.
- 470 Dalgaard JZ, Klar AJ. 2000. *swi1* and *swi3* perform imprinting, pausing, and termination of DNA
471 replication in *S. pombe*. *Cell* **102**: 745-751.
- 472 David FP, Delafontaine J, Carat S, Ross FJ, Lefebvre G, Jarosz Y, Sinclair L, Noordermeer D, Rougemont J,
473 Leleu M. 2014. HTSstation: a web application and open-access libraries for high-throughput
474 sequencing data analysis. *PLoS One* **9**: e85879.
- 475 De Piccoli G, Katou Y, Itoh T, Nakato R, Shirahige K, Labib K. 2012. Replisome stability at defective DNA
476 replication forks is independent of S phase checkpoint kinases. *Mol Cell* **45**: 696-704.
- 477 Di Felice F, Cioci F, Camilloni G. 2005. FOB1 affects DNA topoisomerase I *in vivo* cleavages in the
478 enhancer region of the *Saccharomyces cerevisiae* ribosomal DNA locus. *Nucleic Acids Res* **33**:
479 6327-6337.
- 480 Duguet M. 1997. When helicase and topoisomerase meet! *J Cell Sci* **110 (Pt 12)**: 1345-1350.
- 481 Fiorani S, Mimun G, Caleca L, Piccini D, Pelliccioli A. 2008. Characterization of the activation domain of the
482 Rad53 checkpoint kinase. *Cell Cycle* **7**: 493-499.
- 483 Foss EJ. 2001. Toflp regulates DNA damage responses during S phase in *Saccharomyces cerevisiae*.
484 *Genetics* **157**: 567-577.
- 485 Gadaleta MC, Noguchi E. 2017. Regulation of DNA Replication through Natural Impediments in the
486 Eukaryotic Genome. *Genes (Basel)* **8**.
- 487 Gaillard H, Garcia-Muse T, Aguilera A. 2015. Replication stress and cancer. *Nat Rev Cancer* **15**: 276-289.

- 488 Gambus A, Jones RC, Sanchez-Diaz A, Kanemaki M, van Deursen F, Edmondson RD, Labib K. 2006. GINS
489 maintains association of Cdc45 with MCM in replisome progression complexes at eukaryotic
490 DNA replication forks. *Nat Cell Biol* **8**: 358-366.
- 491 Haruki H, Nishikawa J, Laemmli UK. 2008. The anchor-away technique: rapid, conditional establishment
492 of yeast mutant phenotypes. *Mol Cell* **31**: 925-932.
- 493 Hizume K, Endo S, Muramatsu S, Kobayashi T, Araki H. 2018. DNA polymerase epsilon-dependent
494 modulation of the pausing property of the CMG helicase at the barrier. *Genes Dev* **32**: 1315-
495 1320.
- 496 Hodgson B, Calzada A, Labib K. 2007. Mrc1 and Tof1 regulate DNA replication forks in different ways
497 during normal S phase. *Mol Biol Cell* **18**: 3894-3902.
- 498 Hosono Y, Abe T, Higuchi M, Kajii K, Sakuraba S, Tada S, Enomoto T, Seki M. 2014. Tipin functions in the
499 protection against topoisomerase I inhibitor. *J Biol Chem* **289**: 11374-11384.
- 500 Ivessa AS, Lenzmeier BA, Bessler JB, Goudsouzian LK, Schnakenberg SL, Zakian VA. 2003. The
501 *Saccharomyces cerevisiae* helicase Rrm3p facilitates replication past nonhistone protein-DNA
502 complexes. *Mol Cell* **12**: 1525-1536.
- 503 Ivessa AS, Zhou JQ, Zakian VA. 2000. The *Saccharomyces* Pif1p DNA helicase and the highly related
504 Rrm3p have opposite effects on replication fork progression in ribosomal DNA. *Cell* **100**: 479-
505 489.
- 506 Kaeberlein M, McVey M, Guarente L. 1999. The SIR2/3/4 complex and SIR2 alone promote longevity in
507 *Saccharomyces cerevisiae* by two different mechanisms. *Genes Dev* **13**: 2570-2580.
- 508 Keszthelyi A, Minchell NE, Baxter J. 2016. The Causes and Consequences of Topological Stress during
509 DNA Replication. *Genes (Basel)* **7**.
- 510 Kim RA, Wang JC. 1989a. Function of DNA topoisomerases as replication swivels in *Saccharomyces*
511 *cerevisiae*. *J Mol Biol* **208**: 257-267.
- 512 -. 1989b. A subthreshold level of DNA topoisomerases leads to the excision of yeast rDNA as
513 extrachromosomal rings. *Cell* **57**: 975-985.
- 514 Kobayashi T, Horiuchi T, Tongaonkar P, Vu L, Nomura M. 2004. SIR2 regulates recombination between
515 different rDNA repeats, but not recombination within individual rRNA genes in yeast. *Cell* **117**:
516 441-453.
- 517 Krawczyk C, Dion V, Schar P, Fritsch O. 2014. Reversible Top1 cleavage complexes are stabilized strand-
518 specifically at the ribosomal replication fork barrier and contribute to ribosomal DNA stability.
519 *Nucleic Acids Res* **42**: 4985-4995.
- 520 Lang AB, John Peter AT, Walter P, Kornmann B. 2015. ER-mitochondrial junctions can be bypassed by
521 dominant mutations in the endosomal protein Vps13. *J Cell Biol* **210**: 883-890.
- 522 Lou H, Komata M, Katou Y, Guan Z, Reis CC, Budd M, Shirahige K, Campbell JL. 2008. Mrc1 and DNA
523 polymerase epsilon function together in linking DNA replication and the S phase checkpoint. *Mol*
524 *Cell* **32**: 106-117.
- 525 Mattarocci S, Shyian M, Lemmens L, Damay P, Altintas DM, Shi T, Bartholomew CR, Thoma NH, Hardy
526 CF, Shore D. 2014. Rif1 controls DNA replication timing in yeast through the PP1 phosphatase
527 Glc7. *Cell Rep* **7**: 62-69.
- 528 McFarlane RJ, Mian S, Dalgaard JZ. 2010. The many facets of the Tim-Tipin protein families' roles in
529 chromosome biology. *Cell Cycle* **9**: 700-705.

- 530 Mohanty BK, Bairwa NK, Bastia D. 2006. The Tof1p-Csm3p protein complex counteracts the Rrm3p
531 helicase to control replication termination of *Saccharomyces cerevisiae*. *Proc Natl Acad Sci U S A*
532 **103**: 897-902.
- 533 Morawska M, Ulrich HD. 2013. An expanded tool kit for the auxin-inducible degron system in budding
534 yeast. *Yeast* **30**: 341-351.
- 535 Mundbjerg K, Jorgensen SW, Fredsoe J, Nielsen I, Pedersen JM, Bentsen IB, Lisby M, Bjergbaek L,
536 Andersen AH. 2015. Top2 and Sgs1-Top3 Act Redundantly to Ensure rDNA Replication
537 Termination. *PLoS Genet* **11**: e1005697.
- 538 Park H, Sternglanz R. 1999. Identification and characterization of the genes for two topoisomerase I-
539 interacting proteins from *Saccharomyces cerevisiae*. *Yeast* **15**: 35-41.
- 540 Pasero P, Bensimon A, Schwob E. 2002. Single-molecule analysis reveals clustering and epigenetic
541 regulation of replication origins at the yeast rDNA locus. *Genes Dev* **16**: 2479-2484.
- 542 Pommier Y, Sun Y, Huang SN, Nitiss JL. 2016. Roles of eukaryotic topoisomerases in transcription,
543 replication and genomic stability. *Nat Rev Mol Cell Biol* **17**: 703-721.
- 544 Redon C, Pilch DR, Bonner WM. 2006. Genetic analysis of *Saccharomyces cerevisiae* H2A serine 129
545 mutant suggests a functional relationship between H2A and the sister-chromatid cohesion
546 partners Csm3-Tof1 for the repair of topoisomerase I-induced DNA damage. *Genetics* **172**: 67-
547 76.
- 548 Reid RJ, Gonzalez-Barrera S, Sunjevaric I, Alvaro D, Ciccone S, Wagner M, Rothstein R. 2011. Selective
549 ploidy ablation, a high-throughput plasmid transfer protocol, identifies new genes affecting
550 topoisomerase I-induced DNA damage. *Genome Res* **21**: 477-486.
- 551 Schalbetter SA, Mansoubi S, Chambers AL, Downs JA, Baxter J. 2015. Fork rotation and DNA
552 precatenation are restricted during DNA replication to prevent chromosomal instability. *Proc*
553 *Natl Acad Sci U S A* **112**: E4565-4570.
- 554 Shyian M, Mattarocci S, Albert B, Hafner L, Lezaja A, Costanzo M, Boone C, Shore D. 2016. Budding Yeast
555 Rif1 Controls Genome Integrity by Inhibiting rDNA Replication. *PLoS Genet* **12**: e1006414.
- 556 Simon AC, Zhou JC, Perera RL, van Deursen F, Evrin C, Ivanova ME, Kilkenny ML, Renault L, Kjaer S,
557 Matak-Vinkovic D et al. 2014. A Ctf4 trimer couples the CMG helicase to DNA polymerase alpha
558 in the eukaryotic replisome. *Nature* **510**: 293-297.
- 559 Strumberg D, Pilon AA, Smith M, Hickey R, Malkas L, Pommier Y. 2000. Conversion of topoisomerase I
560 cleavage complexes on the leading strand of ribosomal DNA into 5'-phosphorylated DNA
561 double-strand breaks by replication runoff. *Mol Cell Biol* **20**: 3977-3987.
- 562 Teves SS, Henikoff S. 2014. Transcription-generated torsional stress destabilizes nucleosomes. *Nat Struct*
563 *Mol Biol* **21**: 88-94.
- 564 Tourriere H, Versini G, Cordon-Preciado V, Alabert C, Pasero P. 2005. Mrc1 and Tof1 promote replication
565 fork progression and recovery independently of Rad53. *Mol Cell* **19**: 699-706.
- 566 Valjavec-Gratian M, Henderson TA, Hill TM. 2005. Tus-mediated arrest of DNA replication in *Escherichia*
567 *coli* is modulated by DNA supercoiling. *Mol Microbiol* **58**: 758-773.
- 568 van Loenhout MT, de Grunt MV, Dekker C. 2012. Dynamics of DNA supercoils. *Science* **338**: 94-97.
- 569 Voineagu I, Narayanan V, Lobachev KS, Mirkin SM. 2008. Replication stalling at unstable inverted
570 repeats: interplay between DNA hairpins and fork stabilizing proteins. *Proc Natl Acad Sci U S A*
571 **105**: 9936-9941.

572 Yeeles JT, Janska A, Early A, Diffley JF. 2017. How the Eukaryotic Replisome Achieves Rapid and Efficient
573 DNA Replication. *Mol Cell* **65**: 105-116.

574

Shyian_Fig1

bioRxiv preprint doi: <https://doi.org/10.1101/738328>; this version posted August 19, 2019. The copyright holder for this preprint (which was not certified by peer review) is the author/funder. All rights reserved. No reuse allowed without permission.

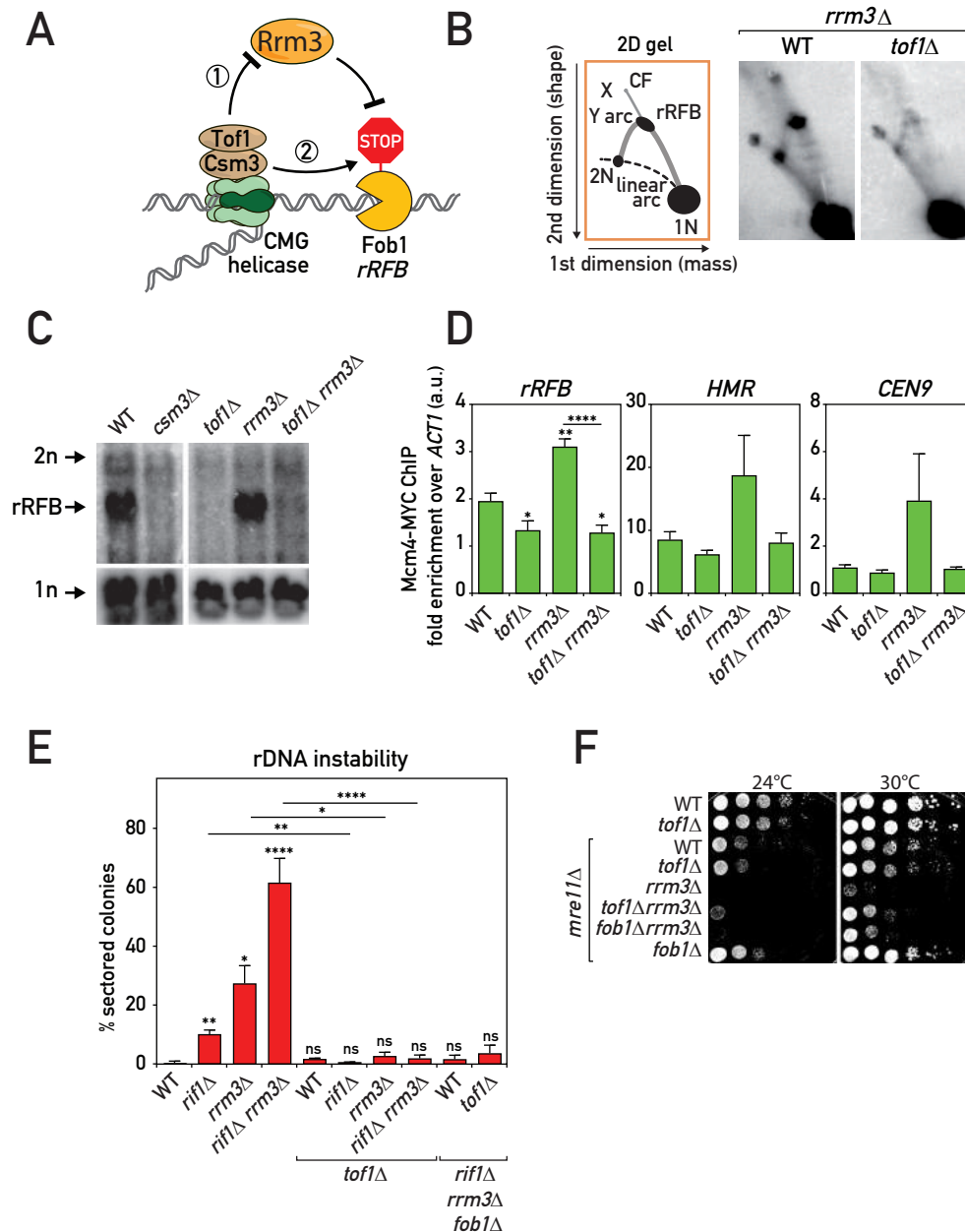


Figure 1. Tof1-Csm3 complex functions independently of Rrm3 helicase (A) Schematics of Rrm3-dependent ('1') and -independent ('2') mechanisms for Tof1-Csm3 role in replication fork pausing at proteinaceous barriers. (B-D) *tof1Δ* suppressed fork pausing in *rrm3Δ* cells: (B) Schematic (left) and representative images (right) of replication intermediates detected in the asynchronous cultures of strains of indicated genotypes by Southern hybridization with rDNA rRFB probe on *Bgl* II-digested DNA separated with 2D gels and blotted to nylon membrane; (C) same as in (B) but Southern blot done directly on 1st dimension gels; (D) Replisome pausing detection with Mcm4-MYC ChIP-qPCR at several pausing sites in asynchronous cultures of strains of the designated genotypes. (E) *tof1Δ* suppressed rDNA instability in *rrm3Δ* and *rif1Δ* cells – rDNA instability measurement with *ADE2* marker loss assay. (F) *tof1Δ* partially alleviated *mre11Δ rrm3Δ* synthetic sickness – serial dilution growth assay. X – X-shaped molecules; CF – converging forks. Means with SEM are plotted; Welch's t test was used for quantitative comparisons (* $p < 0.05$; ** $p < 0.01$; *** $p < 0.001$; **** $p < 0.0001$; ns – not significant). See also Fig. S1.

Shyian_Fig2

bioRxiv preprint doi: <https://doi.org/10.1101/738328>; this version posted August 19, 2019. The copyright holder for this preprint (which was not certified by peer review) is the author/funder. All rights reserved. No reuse allowed without permission.

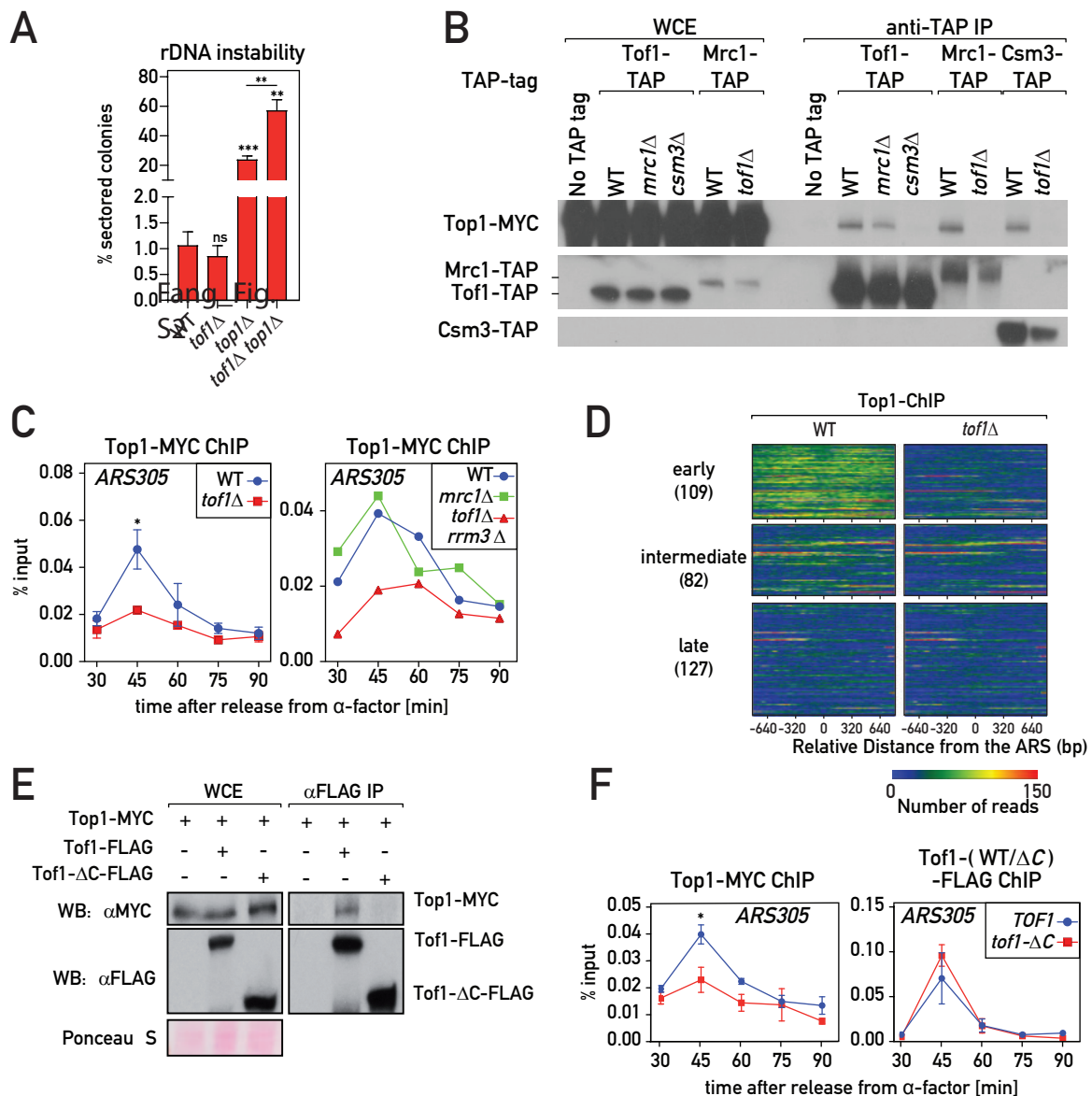


Figure 2. Tof1-Csm3-dependent recruitment of Top1 to the replisome (A) *tof1*Δ did not suppress *top1*Δ-induced rDNA instability, as measured with *ADE2* marker loss assay. (B) Top1 was co-immunoprecipitated with MTC complex in a Tof1- and Csm3-dependent but Mrc1-independent manner. (C-D) Chromatin DNA immunoprecipitated with Top1-MYC from cell cultures synchronously released into S phase from G1 (α -factor) arrest was: (C) subjected to qPCR on *ARS305*; (D) immunoprecipitated DNA from 45' time point (early S phase) was Illumina sequenced, reads mapping to early, intermediate and late origins are shown as a heat map. (E-F) Tof1 lacking C-terminus (*tof1*- Δ C strains) did not co-immunoprecipitate Top1-MYC (E) and was defective in Top1-MYC association with *ARS305* during S phase (F). Here and on subsequent figures: *TOF1* = *TOF1-3xFLAG*; *tof1*- Δ C = *tof1*- Δ 981-1238-3xFLAG. Values plotted and statistics as in Fig. 1. See also Fig. S2.

Shyian_Fig3

bioRxiv preprint doi: <https://doi.org/10.1101/738328>; this version posted August 19, 2019. The copyright holder for this preprint (which was not certified by peer review) is the author/funder. All rights reserved. No reuse allowed without permission.

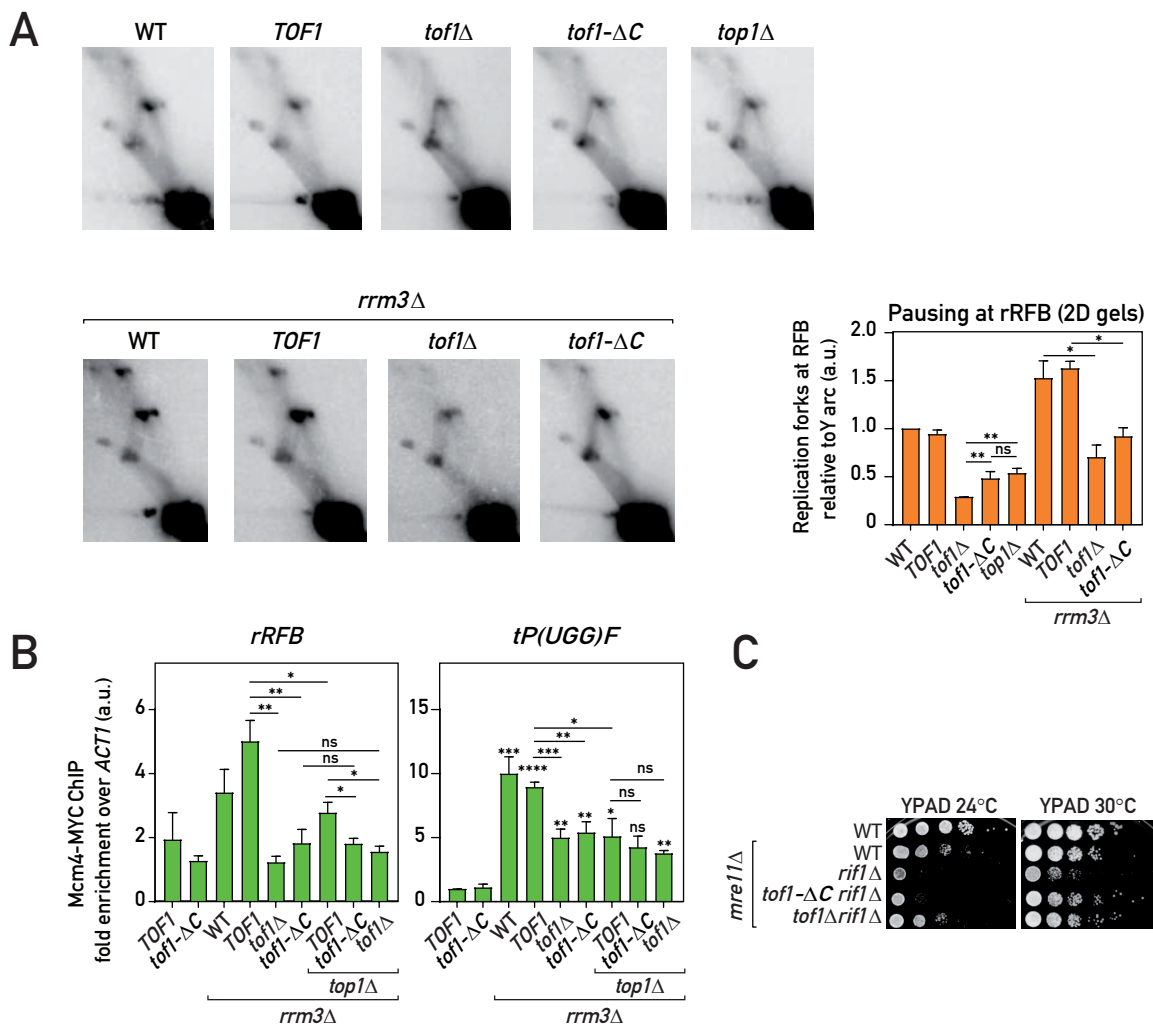


Figure 3. *Tof1*-C-dependent recruitment of Top1 to the replisome promotes fork pausing (A) Replication fork pausing at rRFB measured by 2D gels (as in Fig. 1B) in the strains of indicated genotypes: representative gel images and quantification (pausing in WT = 1, see Materials and Methods). (B) Replisome pausing at rRFB and a tRNA gene (*tP(UGG)F*) detected with Mcm4-MYC ChIP-qPCR in asynchronous cultures. (C) *Tof1*- Δ C is less toxic in *rif1* Δ *mre11* Δ cells than wild type *Tof1*. Values plotted and statistics as in Fig. 1. See also Fig. S3.

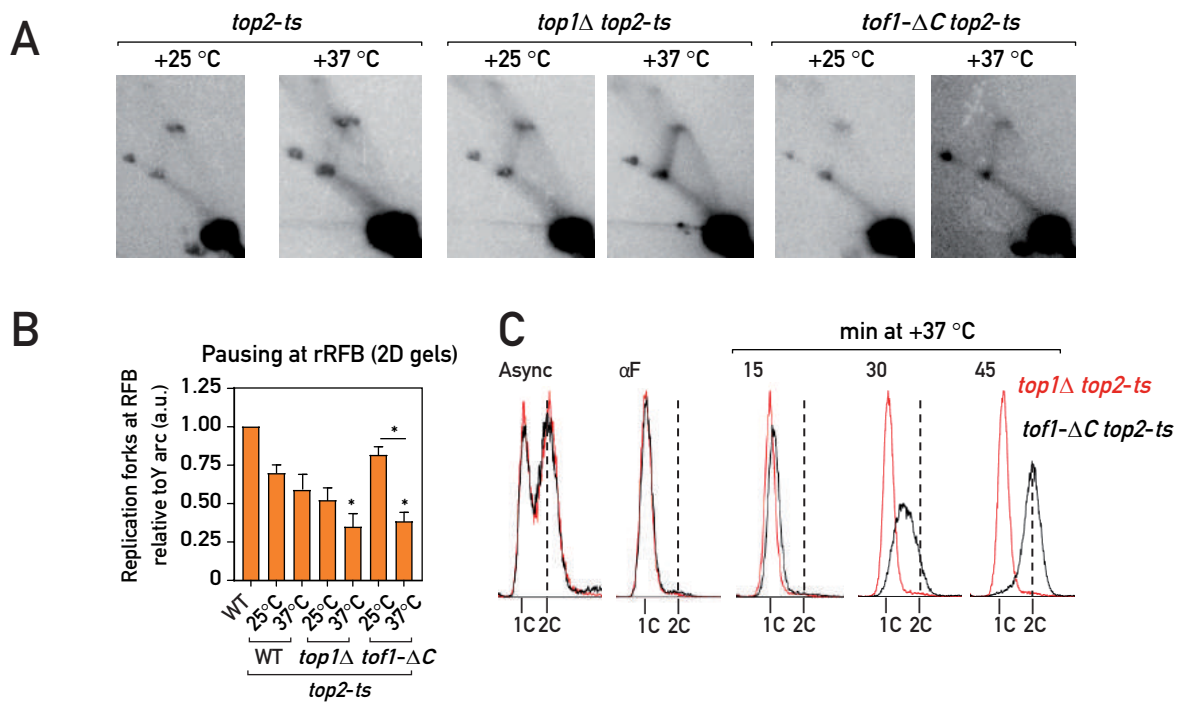


Figure 4. Top2 partially compensates for the fork pausing upon Top1 loss from the replisome (A-B) 2D agarose gel Southern blots (as in Fig. 1B): representative images (A) and quantification (B; pausing in WT = 1, see Materials and Methods) of replication intermediates in asynchronous cultures of the strains of indicated genotypes cultured continuously at +25 °C or transferred for 1 hour to +37 °C. (C) Flow cytometry DNA content profile of the *top1Δ top2-ts* (red) and *tof1-ΔC top2-ts* (black) strains upon release in S phase at +37 °C from G1 (α F) arrest. Values plotted and statistics as in Fig. 1. Stars indicate P values for comparison with *top2-ts* strain at +25 °C. See also Fig. S4.

Shyian_Fig5

bioRxiv preprint doi: <https://doi.org/10.1101/738328>; this version posted August 19, 2019. The copyright holder for this preprint (which was not certified by peer review) is the author/funder. All rights reserved. No reuse allowed without permission.

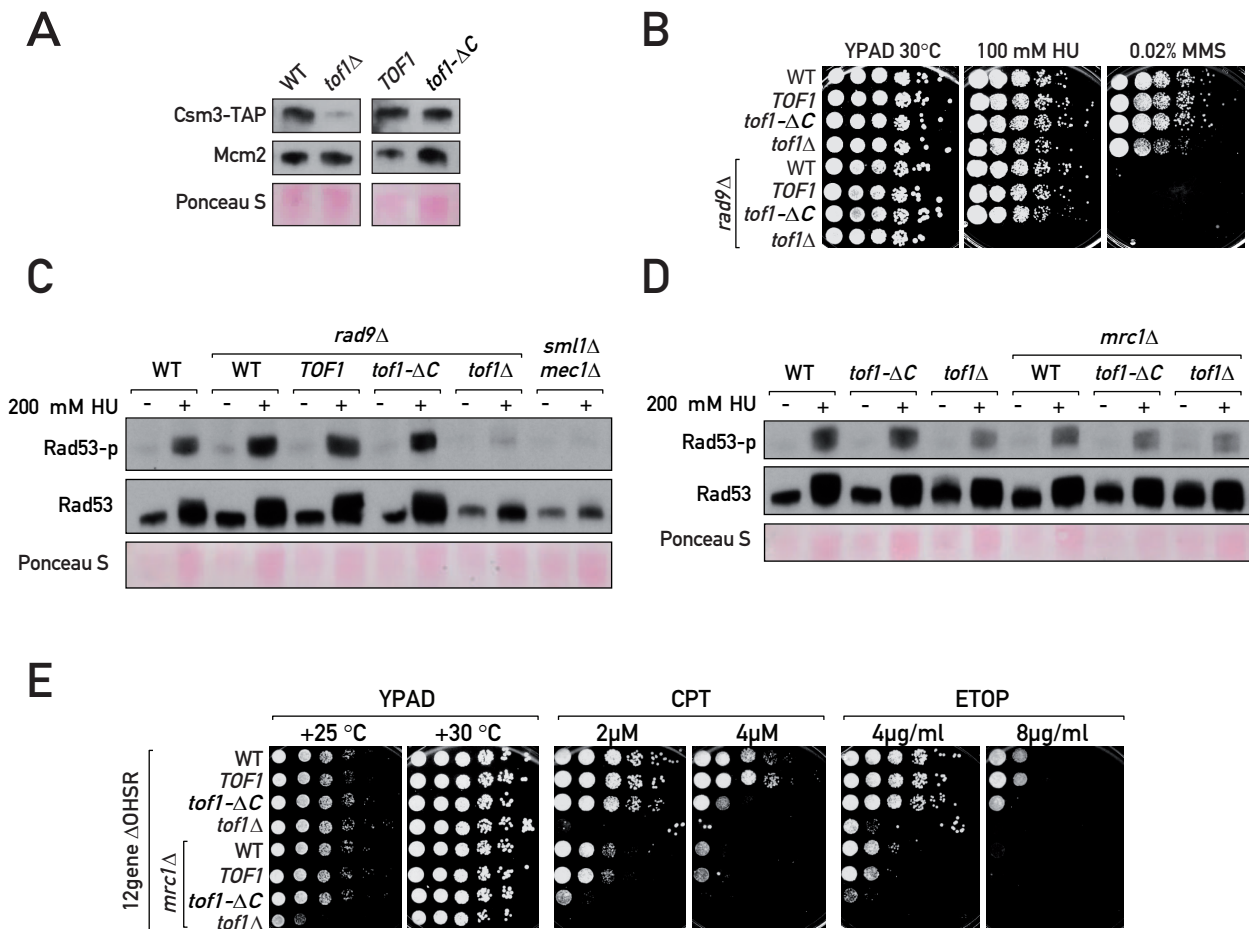


Figure 5. Fork pausing is a separable function of Tof1-Csm3 (A, C-D) Western blotting of TCA-extracted proteins. (A) In contrast to *tof1* Δ , *tof1*- Δ C cells do not degrade Csm3-TAP. (B, E) Serial dilution growth assays. (B) Tof1- Δ C supports viability of *rad9* Δ cells under hydroxyurea (HU) treatment. (C-D) Tof1- Δ C is proficient in DRC activation under HU treatment. (E) Mrc1 supports *tof1*- Δ C cells survival under topoisomerase-blocking damage. CPT – camptothecin; ETOP – etoposide; MMS – methyl methanesulfonate; 12gene Δ OHSR – multidrug sensitive yeast background. See also Fig. S5.

Shyian_Fig6

bioRxiv preprint doi: <https://doi.org/10.1101/738328>; this version posted August 19, 2019. The copyright holder for this preprint (which was not certified by peer review) is the author/funder. All rights reserved. No reuse allowed without permission.

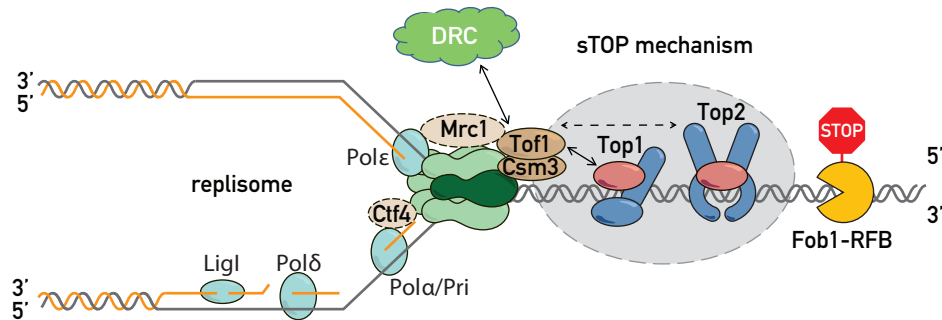


Figure 6. Replisome ‘sTOP’ model (‘slowing down with TOPoisomerases I-II’) Tof1-Csm3 promotes replication fork pausing at proteinaceous barriers via topoisomerase I (and II, dashed line with arrows), either by recruiting topoisomerases to the replisome or/and by recognizing topoisomerases bound in front of the fork. sTOP function of Tof1-Csm3 is distinct from its Mrc1-shared role in DRC (DNA replication checkpoint). See text for details.

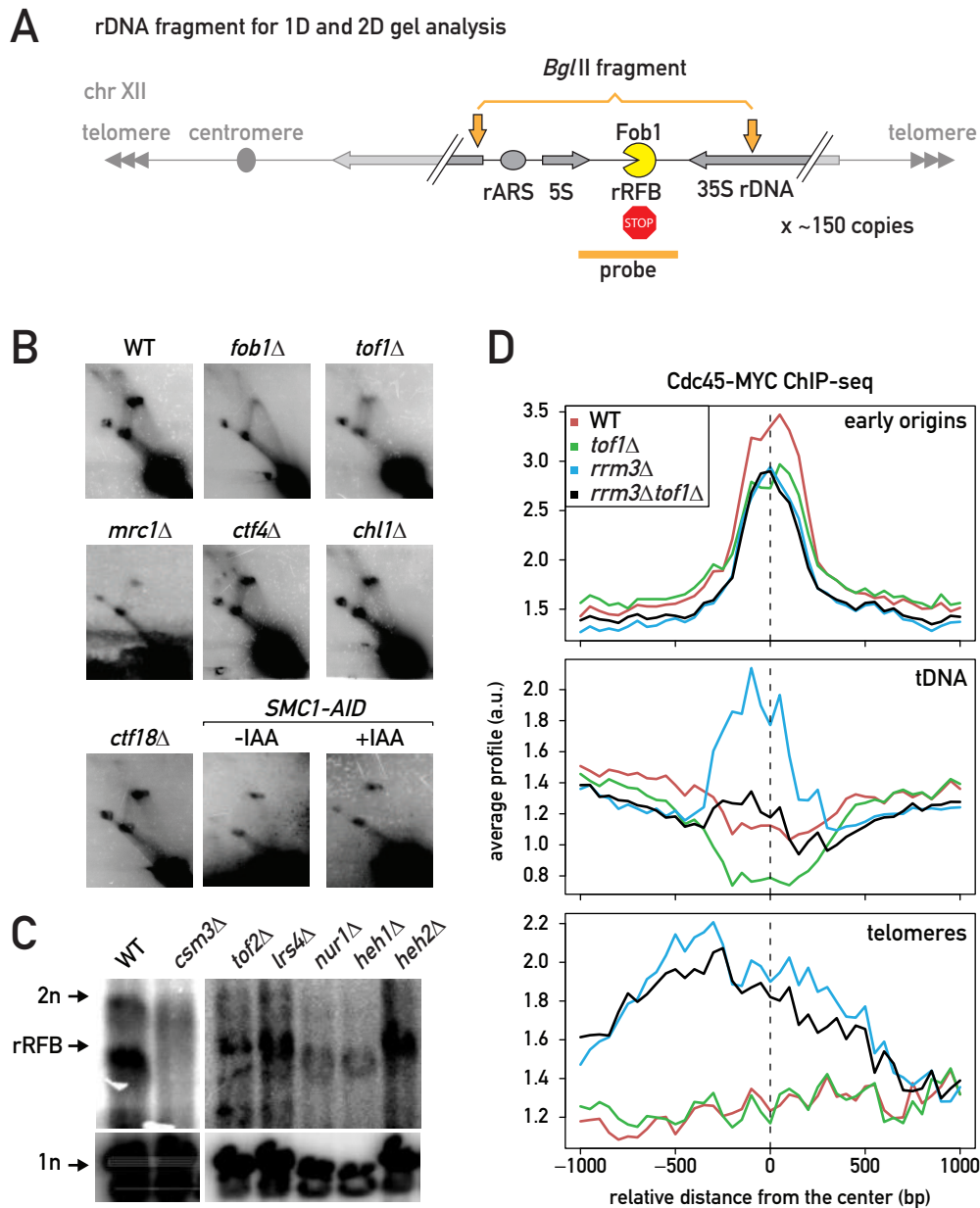


Figure S1. Related to Figure 1. Tof1-Csm3 complex functions independently of cohesion, peripheral anchoring and Rrm3 helicase (A) Diagram of the rDNA locus with the analyzed BglII fragment and location of the probe (rRFB) used for Southern blot hybridization of the 1D and 2D gels. (B) 2D gels for the estimation of fork pausing at rRFB in deletion mutants of the Replisome Progression Complex and sister chromatid cohesion establishment factors (*TOF1*, *MRC1*, *CTF4*, *CHL1*, and *CTF18*) and upon cohesin degradation with auxin (*SMC1-AID*). See Figure 1B for the diagram explaining DNA species on 2D gels. (C) 1D gels for the estimation of fork pausing at rRFB in deletion mutants of factors mediating peripheral anchoring of rDNA repeats to the nuclear envelope (cohibin and CLIP complexes). (D) Cdc45-MYC ChIP-seq in asynchronously growing cultures. Aggregation plots of the anti-MYC ChIP signal in Cdc45-MYC vs anti-MYC ChIP signal in WT not tagged control centered on early origins, tRNA genes and telomeres are shown.

Shyian_FigS2

bioRxiv preprint doi: <https://doi.org/10.1101/738328>; this version posted August 19, 2019. The copyright holder for this preprint (which was not certified by peer review) is the author/funder. All rights reserved. No reuse allowed without permission.

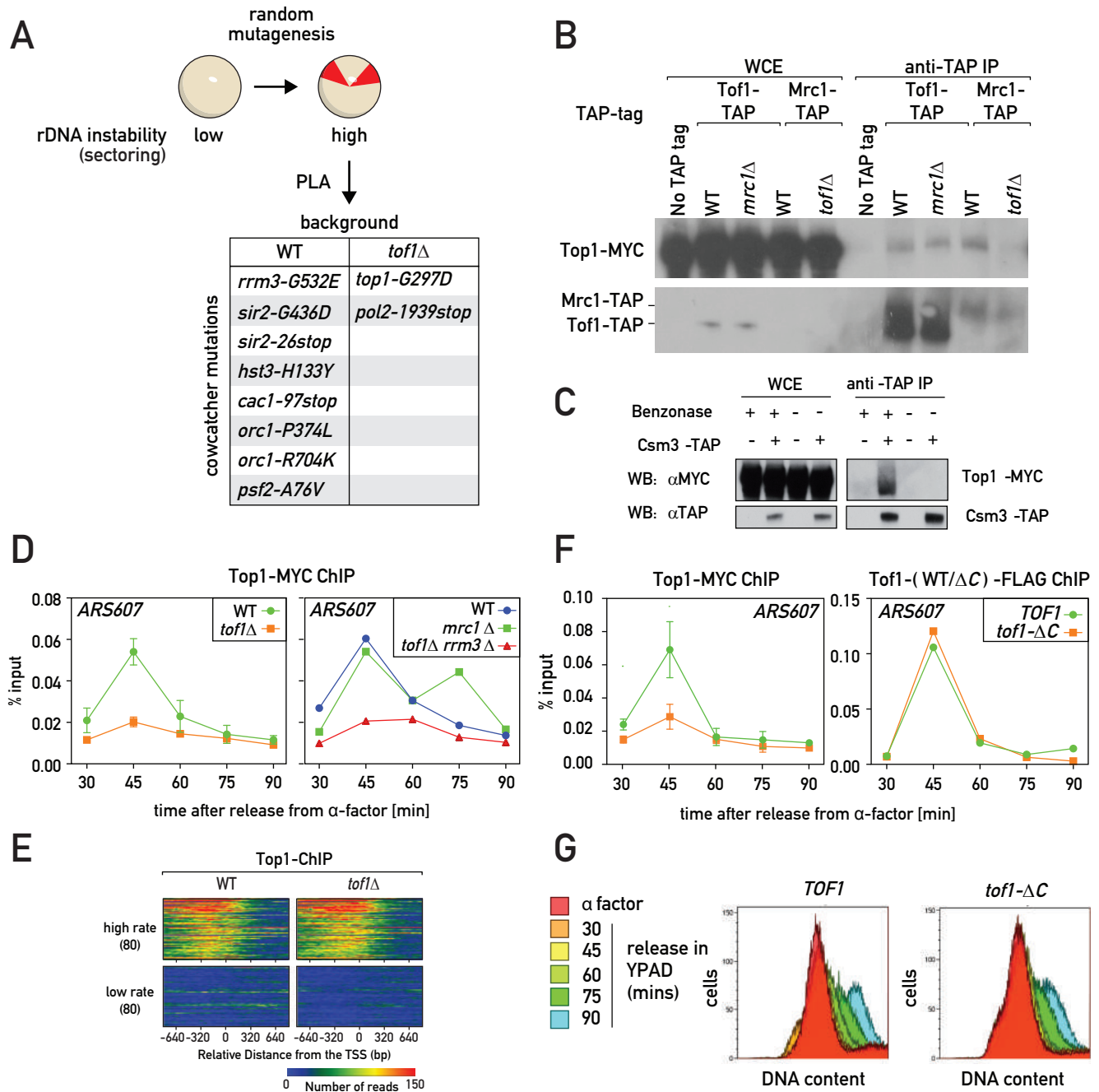


Figure S2. Related to Figure 2. Tof1-Csm3 recruits Top1 to the replisome (A) An outline of the “cowcatcher” screen and mutants identified by Pooled Linkage Analysis (PLA) as leading to elevated rDNA instability in WT and *tof1*Δ backgrounds. (B-C) Western blot detection of the Top1-MYC in Tof1-TAP and Mrc1-TAP (B) or Csm3-TAP (C) anti-TAP immunoprecipitates; DNA degradation by Benzonase was absolutely required to co-immunoprecipitate Top1 (C). (D-G) ChIP followed by qPCR at *ARS607* or high throughput sequencing of Top1-MYC and Tof1- or Tof1-ΔC-FLAG in cell cultures synchronously released in S phase from G1 (α-factor) arrest: Top1-MYC ChIP-qPCR in the strains of designated genotypes (D); distribution of reads mapped to transcription start sites (TSS) is similar in WT and *tof1*Δ cells (E); Top1-MYC (left panel) or Tof1-FLAG and Tof1-ΔC-FLAG (right panel) ChIP-qPCR in *TOF1* and *tof1*-ΔC cells (F); flow cytometry profiles in *TOF1* WT and *tof1*-ΔC cells (for the experiment depicted on the Figure 2F and S2F) (G).

Shyian_FigS3

bioRxiv preprint doi: <https://doi.org/10.1101/738328>; this version posted August 19, 2019. The copyright holder for this preprint (which was not certified by peer review) is the author/funder. All rights reserved. No reuse allowed without permission.

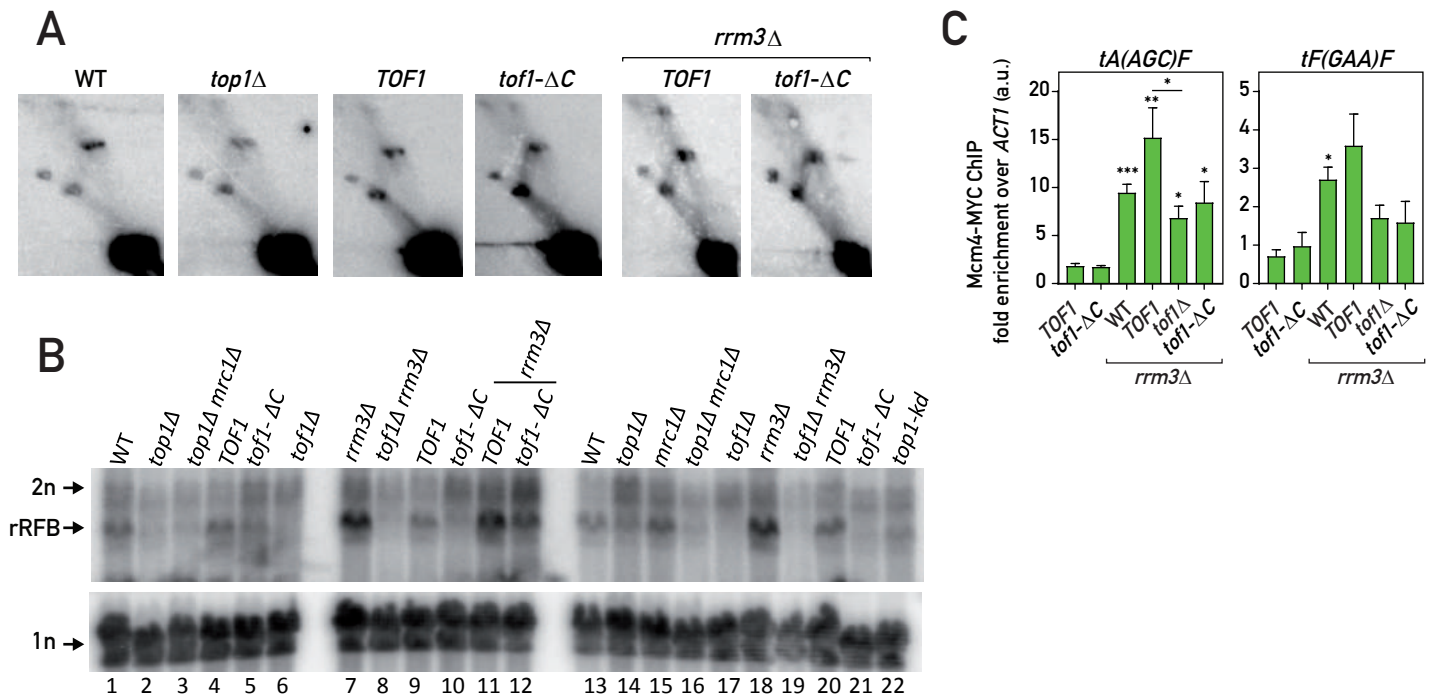


Figure S3. Related to Figure 3. Tof1-C with Top1 promote fork pausing (A-B) 2D gels (A) and 1D gels (B) of the *Bgl* II digested DNA isolated from asynchronous cell cultures and probed with rDNA rRFB probe. (C) Mcm4-MYC ChIP-qPCR in the asynchronous cultures of the strains of indicated genotypes for two tRNA genes. *top1-kd* – catalytically dead Top1 (*top1-Y727F*). Values plotted and statistics as in Figure 1.

Shyian_FigS4

bioRxiv preprint doi: <https://doi.org/10.1101/738328>; this version posted August 19, 2019. The copyright holder for this preprint (which was not certified by peer review) is the author/funder. All rights reserved. No reuse allowed without permission.

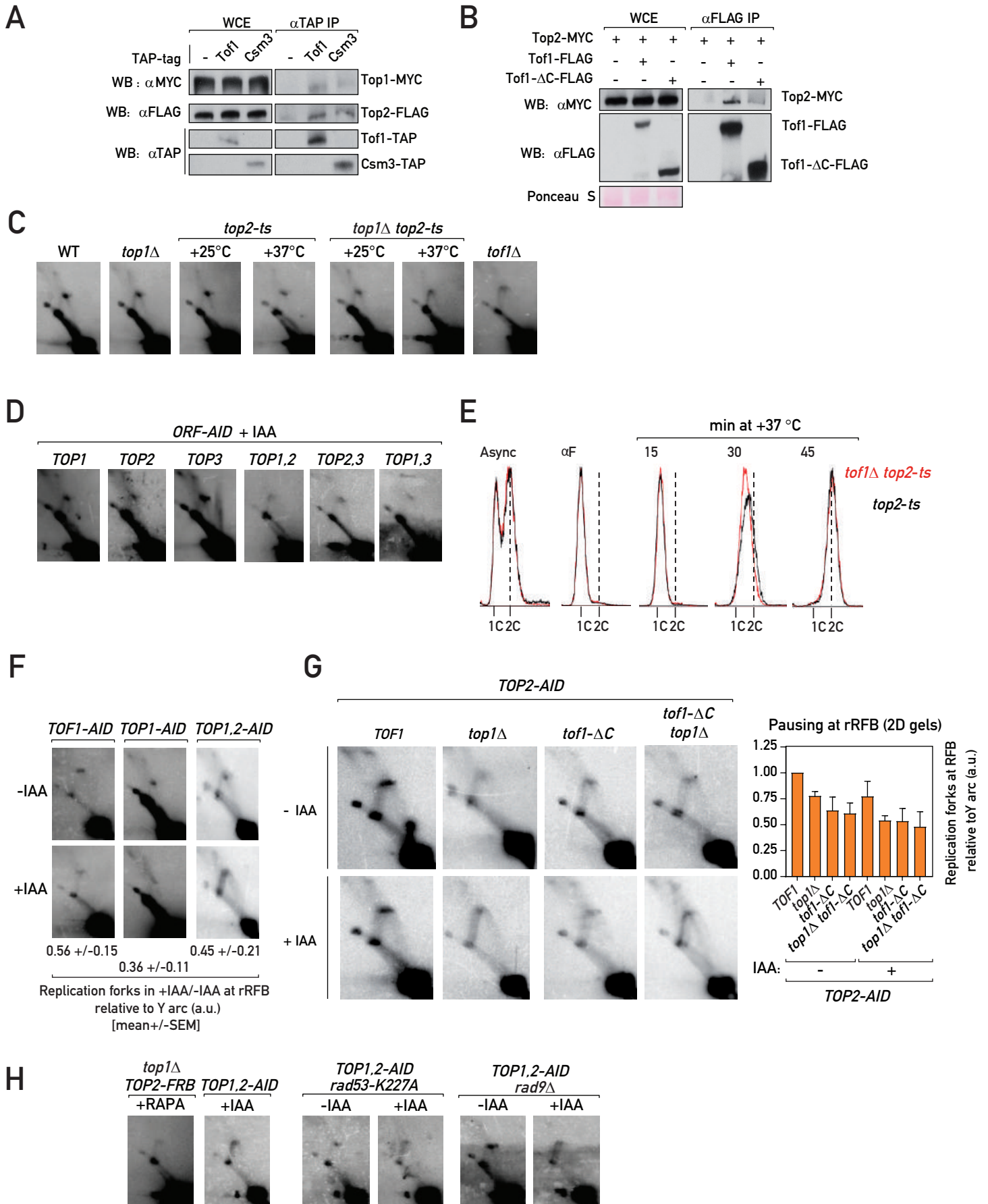


Figure S4. Related to Figure 4. Tof1-Csm3 engages Top1 and Top2 to pause the replisome (A-B) Co-immunoprecipitation experiments: Immunoprecipitates of Tof1 and Csm3 contained Top1 and Top2 (A), Top2 in the immunoprecipitates of Tof1-FLAG and Tof1- Δ C-FLAG (B). (C-D) 2D gels of the *Bgl* II digested DNA isolated from asynchronous cell cultures and probed with rDNA rRFB probe: DNA from asynchronous cultures of control strains (grown at +30 °C) or *top2-ts* strains (grown at +25 °C and shifted or not to +37 °C for 1 hour) (C); DNA from strains harboring AID-tagged topoisomerase genes *TOP1*, *TOP2* and *TOP3* from asynchronous cultures treated for 1 hour with 1 mM IAA (Indole-3-acetic acid) to degrade respective proteins (D). (E) Flow cytometry DNA content profile of the *tof1* Δ *top2-ts* (red) and *top2-ts* (black) strains upon release in S phase at +37 °C from G1 (α F) arrest. (F-H) 2D gels as in Figure S4D): upon Tof1, Top1 or Top1 and Top2 degradation (F); upon Top2 degradation (left panel – representative images; right panel – quantifications) (G); fork pausing in strains additionally harboring mutations of the DNA damage checkpoint genes (*rad53-K227A* and *rad9* Δ) (H). Values plotted and statistics as in Figure 1.

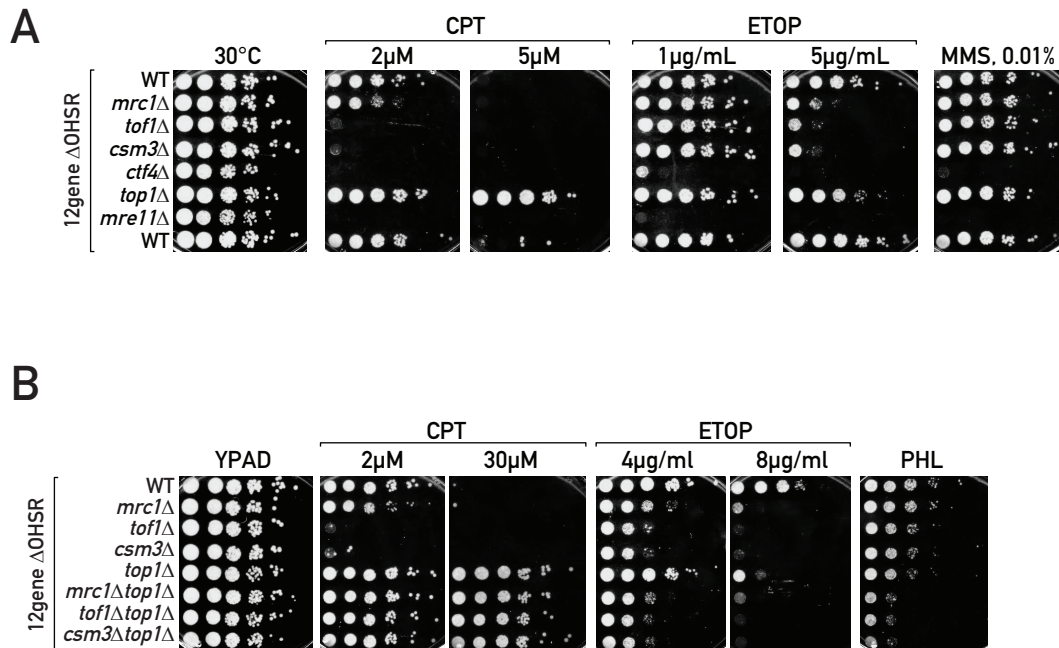


Figure S5. Related to Figure 5. Fork pausing complex protects cells from topoisomerase-blocking agents (A-B) Serial dilution growth assays: in mutants of replication fork progression complex (A) and in combinations of MTC genes deletion mutants and *top1* Δ . Genotoxic agents: CPT – camptothecin; ETOP – etoposide, MMS – methyl methanesulfonate (alkylating agent), PHL – phleomycin (used at 20 μ g/mL; DSB-inducing agent).

Table S1. Yeast strains used in this study

Strain	Genotype	Figures	Source
YDS2	<i>W303 (leu2-3,112 trp1-1 can1-100 ura3-1 ade2-1 his3-11,15) MATa WT</i>	4A, 4B, 3C	Lab collection
OTA017	<i>12geneΔ0HSR (multidrug-sensitive yeast background) MATa</i>		(Chinen et al., 2011)
YMS1294 (5-1)	<i>W303 MATa RAD5+ bar1Δ MCM4-13MYC::HIS3MX6 rrm3Δ::HPHMX4</i>	1B, 1D, 3A 3B, S3C	This study
YMS1299-13	<i>W303 MATa RAD5+ bar1Δ MCM4-13MYC::HIS3MX6 rrm3Δ::HPHMX4 tof1Δ::LEU2</i>	1B, 1D, 3A, 3B, S3C	This study
BY4741	<i>BY (MATa his3Δ1 leu2Δ0 met15Δ0 ura3Δ0) MATa WT</i>	1C, S1B, S1C	Lab collection
YMS1610	<i>BY MATa csm3Δ::KANMX</i>	1C, S1C	This study
YMS1266-I	<i>W303 MATa RDN1::ADE2::URA3::TRP1 tof1Δ::HPHMX4</i>	1C, 1E, S1B, S2A	This study
YMS909	<i>W303 MATa RDN1::ADE2 rrm3Δ::KANMX6</i>	1C, 1E	(Shyian et al., 2016)
YMS1282-1	<i>W303 MATa RDN1::ADE2 rrm3Δ::KANMX6 tof1Δ::HIS3MX6</i>	1C	This study
YSM266-4	<i>W303 MATa RAD5+ bar1Δ MCM4-13MYC::HIS3MX6</i>	1D	(Matarrocci et al., 2014)
YMS1289-7	<i>W303 MATa RAD5+ bar1Δ MCM4-13MYC::HIS3MX6 tof1Δ::LEU2</i>	1D	This study
YMS907	<i>W303 MATa RDN1::ADE2</i>	1E	(Shyian et al., 2016)
YMS908	<i>W303 MATa RDN1::ADE2 rif1Δ::NATMX4</i>	1E	(Shyian et al., 2016)
YMS910	<i>W303 MATa RDN1::ADE2 rif1Δ::NATMX4 rrm3Δ::KANMX6</i>	1E	(Shyian et al., 2016)
YMS1228	<i>W303 MATa RDN1::ADE2 rif1Δ::NATMX4 tof1Δ::HPHMX4</i>	1E	This study
YMS1224	<i>W303 MATa RDN1::ADE2 rrm3Δ::KANMX6 tof1Δ::HPHMX4</i>	1E	This study
YMS1226	<i>W303 MATa RDN1::ADE2 rrm3Δ::KANMX6 rif1Δ::NATMX4 tof1Δ::HPHMX4</i>	1E	This study
YMS912	<i>W303 MATa RDN1::ADE2 rif1Δ::NATMX4 rrm3Δ::KANMX6 fob1Δ::URA3</i>	1E	(Shyian et al., 2016)
YMS1227	<i>W303 MATa RDN1::ADE2 rrm3Δ::KANMX6 rif1Δ::NATMX4 tof1Δ::HPHMX4 fob1Δ::URA3</i>	1E	This study
YMS1605-2	<i>W303 MATalpha RDN1::ADE2</i>	2A	This study
YMS1606-2	<i>W303 MATalpha RDN1::ADE2 tof1Δ::HPHMX4</i>	2A	This study
YMS1607-2	<i>W303 MATalpha RDN1::ADE2 top1Δ::NATMX4</i>	2A	This study
YMS1608-2	<i>W303 MATalpha RDN1::ADE2 top1Δ::NATMX4 tof1Δ::HPHMX4</i>	2A	This study
YMS1505	<i>W303 MATa TOP1-13MYC::KANMX3</i>	2B, S2B, S2C	This study
YMS1506	<i>W303 MATa TOP1-13MYC::KANMX3 Tof1-TAP::HIS3</i>	2B, S2B	This study
YMS1507	<i>W303 MATa TOP1-13MYC::KANMX3 Tof1-TAP::HIS3 mrc1Δ::HPHMX4</i>	2B, S2B	This study
YMS1508	<i>W303 MATa TOP1-13MYC::KANMX3 Tof1-TAP::HIS3 csm3Δ::HPHMX4</i>	2B	This study
YMS1512	<i>W303 MATa TOP1-13MYC::KANMX3 Mrc1-TAP::HIS3</i>	2B, S2B	This study
YMS1513	<i>W303 MATa TOP1-13MYC::KANMX3 Mrc1-TAP::HIS3 tof1Δ::HPHMX4</i>	2B, S2B	This study
YMS1510	<i>W303 MATa TOP1-13MYC::KANMX3 Csm3-TAP::HIS3</i>	2B, 5A, S2C	This study
YMS1511	<i>W303 MATa TOP1-13MYC::KANMX3 Csm3-TAP::HIS3 tof1Δ::HPHMX4</i>	2B, 5A	This study
YMS1539-5	<i>W303 MATa RAD5+ bar1Δ Mcm4-3FLAG::KANMX TOP1-13MYC::HIS3MX4</i>	2C, 2D, S2D, S2E	This study
YMS1540-9	<i>W303 MATa RAD5+ bar1Δ Mcm4-3FLAG::KANMX TOP1-</i>	2C, 2D,	This study

	<i>13MYC::HIS3MX4 tof1Δ::LEU2</i>	S2D, S2E	
YMS1555-1	<i>W303 MATa RAD5+ bar1Δ Mcm4-3FLAG::KANMX TOP1-13MYC::HIS3MX4 mrc1Δ::LEU2</i>	2C, 2D, S2D	This study
YMS1542-19	<i>W303 MATa RAD5+ bar1Δ Mcm4-3FLAG::KANMX TOP1-13MYC::HIS3MX4 tof1Δ::LEU2 rrm3Δ::HPHMX4</i>	2C, 2D, S2D	This study
YMS1538	<i>W303 MATa RAD5+ bar1Δ TOP1-13MYC::HIS3MX4</i>	2E	This study
YMS1551-5	<i>W303 MATa RAD5+ bar1Δ TOP1-13MYC::HIS3MX4 TOF1-3FLAG::KANMX</i>	2E, 2F, S2F, S2G	This study
YMS1552-6	<i>W303 MATa RAD5+ bar1Δ TOP1-13MYC::HIS3MX4 tof1-Δ981-1238-3FLAG::KANMX</i>	2E, 2F, S2F, S2G	This study
YMS1449	<i>12geneΔ0HSR MATa</i>	3A, S3A	This study
YMS1638-5	<i>12geneΔ0HSR MATa TOF1-3FLAG::KANMX</i>	3A, S3A	This study
YMS1561-1	<i>12geneΔ0HSR MATa tof1Δ::LEU2</i>	3A, 5B, 5D, 5E, S5B	This study
YMS1639-4	<i>12geneΔ0HSR MATa tof1-Δ981-1238-3FLAG::KANMX</i>	3A, S3A	This study
YMS1563-1	<i>12geneΔ0HSR MATa top1Δ::KANMX6</i>	3A, S3A, S5B	This study
YMS1646-8	<i>W303 MATa RAD5+ bar1Δ MCM4-13MYC::HIS3MX6 rrm3Δ::HPHMX4 TOF1-3FLAG::KANMX</i>	3A, 3B, S3A, 3B, S3C	This study
YMS1647-12	<i>W303 MATa RAD5+ bar1Δ MCM4-13MYC::HIS3MX6 rrm3Δ::HPHMX4 tof1-Δ981-1238-3FLAG::KANMX</i>	3A, 3B, S3A, S3C	This study
YMS1644-1	<i>W303 MATa RAD5+ bar1Δ MCM4-13MYC::HIS3MX6 TOF1-3FLAG::KANMX</i>	3B, S3C	This study
YMS1645-4	<i>W303 MATa RAD5+ bar1Δ MCM4-13MYC::HIS3MX6 tof1-Δ981-1238-3FLAG::KANMX</i>	3B, S3C	This study
YMS1676-13	<i>W303 MATa RAD5+ bar1Δ MCM4-13MYC::HIS3MX6 rrm3Δ::HPHMX4 TOF1-3FLAG::KANMX top1Δ::NATMX4</i>	3B, S3C	This study
YMS1677-15	<i>W303 MATa RAD5+ bar1Δ MCM4-13MYC::HIS3MX6 rrm3Δ::HPHMX4 tof1-Δ981-1238-3FLAG::KANMX top1Δ::NATMX4</i>	3B, S3C	This study
YMS1673-7	<i>W303 MATa RAD5+ bar1Δ MCM4-13MYC::HIS3MX6 rrm3Δ::HPHMX4 tof1Δ::LEU2 top1Δ::NATMX4</i>	3B, S3C	This study
YMS1457	<i>W303 MATalpha top2-ts</i>	4A, 4B	This study
YMS1465	<i>W303 MATa top1Δ::NATMX4 top2-ts</i>	4A, 4B	This study
YMS1637-1	<i>W303 MATalpha top2-ts tof1-Δ981-1238-3FLAG::KANMX</i>	4A, 4B	This study
YMS1692	<i>W303 MATa top2-ts top1Δ::NATMX4 bar1Δ::LEU2</i>	4C	This study
YMS1689	<i>W303 MATa top2-ts tof1-Δ981-1238-3FLAG::KANMX rif1::NATMX4 RDN1::ADE2 bar1Δ::LEU2</i>	4C	This study
YMS1640-7	<i>W303 MATalpha TOP2-AID*-9myc::hphB URA3::TIR1 Csm3-TAP::HIS3 TOF1-3FLAG::KANMX</i>	5A, S4G	This study
YMS1641-8	<i>W303 MATalpha TOP2-AID*-9myc::hphB URA3::TIR1 Csm3-TAP::HIS3 tof1-Δ981-1238-3FLAG::KANMX</i>	5A, S4G	This study
YMS1559-1	<i>12geneΔ0HSR MATa WT</i>	5B, 5D, 5E, S5B	This study
YMS1707-1	<i>12geneΔ0HSR MATa TOF1-3FLAG::KANMX</i>	5B, 5E	This study
YMS1708-1	<i>12geneΔ0HSR MATa tof1-Δ981-1238-3FLAG::KANMX</i>	5B, 5D, 5E	This study
YMS1712	<i>W303 MATa rad9Δ::SpHIS5</i>	5B, 5C	This study
YMS1713	<i>W303 MATa rad9Δ::SpHIS5 TOF1-3FLAG::KANMX</i>	5B, 5C	This study
YMS1714	<i>W303 MATa rad9Δ::SpHIS5 tof1-Δ981-1238-3FLAG::KANMX</i>	5B, 5C	This study
YMS1715	<i>W303 MATa rad9Δ::SpHIS5 tof1Δ::KANMX4</i>	5B, 5C	This study
YMS419-4	<i>W303 MATa RAD5+ bar1Δ SLD3-13MYC::HIS3MX6</i>	5C	(Shyian et al., 2016)
YMS493	<i>W303 MATa RAD5+ bar1Δ SLD3-13MYC::HIS3MX6 sml1Δ::HPHMX4 mec1Δ::KANMX6</i>	5C	(Shyian et al., 2016)
YMS1560-1	<i>12geneΔ0HSR MATa mrc1Δ::LEU2</i>	5D, 5E, S5B	This study
YMS1709-1	<i>12geneΔ0HSR MATa mrc1Δ::LEU2 TOF1-3FLAG::KANMX</i>	5E	This study
YMS1710-1	<i>12geneΔ0HSR MATa mrc1Δ::LEU2 tof1-Δ981-1238-3FLAG::KANMX</i>	5D, 5E	This study

YMS1711-1	<i>12geneΔOHSR MATa mrc1Δ::LEU2 tof1Δ::LEU2</i>	5D, 5E	This study
YMS1024-1	<i>W303 MATa URA3::BrdU-Inc fob1Δ::KANMX6</i>	S1B	(Shyian et al., 2016)
YMS1609	<i>BY MATa tof1Δ::KANMX</i>	S1B	This study
YMS598-2	<i>W303 MAT alpha mrc1Δ::HPHMX4</i>	S1B	This study
YMS1611	<i>BY MATa ctf4Δ::KANMX</i>	S1B	This study
YMS1612	<i>BY MATa chl1Δ::KANMX</i>	S1B	This study
YMS1613	<i>BY MATa ctf18Δ::KANMX</i>	S1B	This study
YMS1403-14	<i>W303 MATa OsTIR1::URA3 SMC1-AID*-9myc::hphB</i>	S1B	This study
YMS1614	<i>BY MATa tof2Δ::KANMX</i>	S1C	This study
YMS1615	<i>BY MATa lrs4Δ::KANMX</i>	S1C	This study
YMS1616	<i>BY MATa nur1Δ::KANMX</i>	S1C	This study
YMS1617	<i>BY MATa heh1Δ::KANMX</i>	S1C	This study
YMS1618	<i>BY MATa heh2Δ::KANMX</i>	S1C	This study
YMS461-2	<i>W303 MATa RAD5+ bar1Δ CDC45-13MYC::HIS3MX6</i>	S1D	This study
YMS1288-3	<i>W303 MATa RAD5+ bar1Δ CDC45-13MYC::HIS3MX6 tof1Δ::LEU2</i>	S1D	This study
YMS1293 (4-1)	<i>W303 MATa RAD5+ bar1Δ CDC45-13MYC::HIS3MX6 rrm3Δ::HPHMX4</i>	S1D	This study
YMS1298-7	<i>W303 MATa RAD5+ bar1Δ CDC45-13MYC::HIS3MX6 rrm3Δ::HPHMX4 tof1Δ::LEU2</i>	S1D	This study
YMS1264-E	<i>W303 MATa RDN1::ADE2::URA3::TRP1 WT</i>	S2A	This study
YMS465-1	<i>W303 MATa mre11Δ::HPHMX4</i>	3C	(Shyian et al., 2016)
YMS467-1	<i>W303 MATa mre11Δ::HPHMX4 rif1Δ::NATMX4</i>	3C	(Shyian et al., 2016)
YMS1703	<i>W303 MATalpha mre11Δ::HPHMX4 rif1Δ::NATMX4 tof1-Δ981-1238-3FLAG::KANMX</i>	3C	This study
YMS1704	<i>W303 MATalpha mre11Δ::HPHMX4 rif1Δ::NATMX4 tof1::KANMX6</i>	3C	This study
YMS1481	<i>W303 MATalpha Top1-MYC::KANMX3</i>	S4A	This study
YMS1482-3	<i>W303 MATalpha Top1-MYC::KANMX3 TOF1-TAP::HIS3</i>	S4A	This study
YMS1483-8	<i>W303 MATalpha Top1-MYC::KANMX3 CSM3-TAP::HIS3</i>	S4A	This study
YMS1485	<i>W303 MATalpha TOP2-3FLAG::KANMX</i>	S4A	This study
YMS1486-5	<i>W303 MATalpha TOP2-3FLAG::KANMX TOF1-TAP::HIS3</i>	S4A	This study
YMS1487-9	<i>W303 MATalpha TOP2-3FLAG::KANMX CSM3-TAP::HIS3</i>	S4A	This study
YMS1496.	<i>W303 MATa RAD5+ bar1Δ TOP2-AID*-9myc::hphB</i>	S4B	This study
YMS1553-9	<i>W303 MATa RAD5+ bar1Δ TOP2-AID*-9myc::hphB TOF1-3FLAG::KANMX</i>	S4B	This study
YMS1554-9	<i>W303 MATa RAD5+ bar1Δ TOP2-AID*-9myc::hphB tof1-Δ981-1238-3FLAG::KANMX</i>	S4B	This study
YDS3	<i>W303 MATalpha WT</i>	S4C	Lab collection
YMS1405	<i>W303 MATalpha OsTIR1::URA3 tof1Δ::LEU2</i>	S4C	This study
BEN3	<i>W303 MATa top1Δ::NATMX4</i>	S4C	This study
BEN16	<i>W303 MATa top2-ts</i>	S4C	This study
BEN10	<i>W303 MATa top2-ts top1Δ::NATMX4</i>	S4C	This study
BEN240	<i>MATa OsTIR1::URA3 HIS3+ ADE2+ TOP1-AID*-9myc::hphB</i>	S4D, S4F	This study
BEN237	<i>MATa OsTIR1::URA3 HIS3+ ADE2+ TOP2-AID*-9myc::hphB</i>	S4D	This study
BEN250	<i>MATa OsTIR1::URA3 HIS3+ ADE2+ TOP3-AID*-9myc::hphB</i>	S4D	This study
BEN242	<i>MATa OsTIR1::URA3 HIS3+ ADE2+ TOP2-AID*-9myc::hphB TOPI-aid(kanMX)</i>	S4D	This study
YMS1470	<i>MATa OsTIR1::URA3 HIS3+ ADE2+ TOP2-AID*-9myc::hphB TOP3-AID*-9myc::hphB</i>	S4D	This study
YMS1477	<i>MATa OsTIR1::URA3 HIS3+ ADE2+ TOP3-AID*-9myc::hphB TOPI-aid(kanMX)</i>	S4D	This study
YMS1687	<i>W303 MATa top2-ts bar1Δ::LEU2</i>	S4E	This study
YMS1691	<i>W303 MATa top2-ts bar1Δ::LEU2 tof1Δ::HPHMX4</i>	S4E	This study
YMS1459	<i>MATalpha OsTIR1::URA3 TOPI-aid(kanMX) TOP2-AID*-9myc::hphB</i>	S4F	This study

YMS1402-40	<i>W303 MATa OsTIR1::URA3 TOF1-AID*-9myc::hphB</i>	S4F	This study
YMS1635	<i>W303 MATalpha TOP2-AID*-9myc::hphB OsTIR1::URA3 Csm3-TAP::HIS3 top1Δ::NATMX4</i>	S4G	This study
YMS1643-11	<i>W303 MATalpha TOP2-AID*-9myc::hphB OsTIR1::URA3 Csm3-TAP::HIS3 tof1-Δ981-1238-3FLAG::KANMX top1Δ::NATMX4</i>	S4G	This study
BEN151	<i>W303 MATa tor1-1 fpr1Δ::NAT RPL13A-2XFKB12::TRP1 top1Δ::HISMX6 TOP2-FRB::KANMX6</i>	S4H	This study
YMS1460	<i>MATa OsTIR1::URA3 TOP1-aid(kanMX) TOP2-AID*-9myc::hphB</i>	S4H	This study
YMS1467	<i>W303 MATalpha OsTIR1::URA3 TOP1-aid(kanMX) TOP2-AID*-9myc::hphB rad53-K227A::KAN</i>	S4H	This study
YMS1468	<i>MATa OsTIR1::URA3 TOP1-aid(kanMX) TOP2-AID*-9myc::hphB rad9Δ::SpHIS5</i>	S4H	This study
YMS1559-2	<i>I2geneΔ0HSR MATalpha WT</i>	S5A	This study
YMS1560-2	<i>I2geneΔ0HSR MATalpha mrc1Δ::LEU2</i>	S5A	This study
YMS1561-2	<i>I2geneΔ0HSR MATalpha tof1Δ::LEU2</i>	S5A	This study
YMS1562-2	<i>I2geneΔ0HSR MATalpha csm3Δ::LEU2</i>	S5A	This study
YMS1563-2	<i>I2geneΔ0HSR MATalpha top1Δ::KANMX6</i>	S5A	This study
YMS1562-1	<i>I2geneΔ0HSR MATa csm3Δ::LEU2</i>	S5B	This study
YMS1564-1	<i>I2geneΔ0HSR MATa top1Δ::KANMX6 mrc1Δ::LEU2</i>	S5B	This study
YMS1565-1	<i>I2geneΔ0HSR MATa top1Δ::KANMX6 tof1Δ::LEU2</i>	S5B	This study
YMS1566-1	<i>I2geneΔ0HSR MATa top1Δ::KANMX6 csm3Δ::LEU2</i>	S5B	This study